LONG GAP PERIPHERAL NERVE RECONSTRUCTION USING DECELLULARIZED NERVE GRAFTS

by

SRIKANTH VASUDEVAN

Presented to the Faculty of the Graduate School of
The University of Texas at Arlington in Partial Fulfillment
of the Requirements
for the Degree of

DOCTOR OF PHILOSOPHY

THE UNIVERSITY OF TEXAS AT ARLINGTON
DECEMBER 2013

ACKNOWLEDGEMENTS

Firstly, I would like to express my deepest gratitude to my advisors Dr. Jonathan Cheng (Plastic Surgery, University of Texas Southwestern Medical Center, Dallas, TX) and Dr. Edward Keefer (Plexon Inc., Dallas, TX) for all I have learned from them and for their continuous support and training in all stages of my PhD research. The comprehensive training has taught me how to express ideas, ask the right question and improve my problem solving skills. I consider myself fortunate to have Jonathan and Ed as my PhD mentors, as their optimistic training and advice helped me secure a Tidmore Neuroscience Graduate Fellowship, which supported part of my research.

I am grateful to Dr. Liping Tang (Supervising Professor, University of Texas at Arlington, Arlington, TX), Dr. Bruce Gnade (University of Texas at Dallas, Dallas, TX) and Dr. Barry Botterman (University of Texas Southwestern Medical Center, Dallas, TX) for serving on my thesis committee and providing insightful suggestion towards improving my research. I would like to thank my colleague, Tabassum Musa (Plexon Inc., Dallas) for her contributions toward my research. I would also like to extend my gratitude to Daniel Hunter (Washington University School of Medicine, St. Louis, MO) for teaching me vital skills used in my research.

Most importantly, I would like to thank my father Mr. A. Vasudevan, mother Mrs. V. Pankaja and my siblings Mr. V. Premanand and Mrs. S Srividya for their unconditional love, faith and support throughout my achievements. I am grateful to my parents for laying my educational foundation, which led to receiving my Doctoral degree. With deepest love, affection and respect, I would like to thank my wife, Vandana Desikan. I was able to complete my research with her love, support and motivation.

November 1, 2013

ABSTRACT

LONG GAP PERIPHERAL NERVE RECONSTRUCTION

USING DECELLULARIZED

NERVE GRAFTS

Srikanth Vasudevan, PhD

The University of Texas at Arlington, 2013

Supervising Professors: Jonathan J. Cheng and Edward W. Keefer

Peripheral nerve injuries that arise as a result of trauma, tumor excision or birth can adversely affect the quality of patient life, leading to lifelong disabilities in some cases. Autologous nerve grafts are the clinical "gold standard" for long gap nerve repair, and allogeneic nerve grafts are considered the next best treatment option. Despite having numerous benefits, autologous nerve grafts are associated with limited supply, longer operation time, risk of infection, painful neuroma formation and most importantly, loss of function at the donor site. Allogeneic nerve grafts require transient immunosuppression, which exposes the patients to risks of infection, toxicity and possible malignancy. To overcome the limitations of current treatment procedures, use of decellularized nerve grafts has been developed as an alternative treatment strategy. The aim of this research is to develop detergent-free decellularized nerve grafts for repair of long gap peripheral nerve defects.

We first developed a detergent-free decellularization technique for producing nerve grafts with appropriate mechanical, structural and biological properties. These decellularized

nerve grafts were tested for functional nerve regeneration at multiple time points with and without exogenous cells in the grafts across a 35 mm long gap defect. Finally, we compared the detergent-free decellularized nerve grafts with a well-established detergent processing method, and found that the detergent-free decellularized nerve grafts without any additional factors was sufficient to promote functional nerve regeneration.

To understand the molecular differences between a regenerative and a non-regenerative nerve injury, we developed a growth vs. no-growth injury model. Difference in histological and molecular profile between the two injuries indicated a difference in response to injury and repair. Data from this work enabled us to select compounds which could potentially be used for improving nerve regeneration.

Finally, we found that the compounds selected from molecular profiling promoted peripheral nerve regeneration. We optimized the detergent-free decellularization process and examined nerve regeneration with and without addition of exogenous compounds. The *in vivo* results suggest that the improved decellularized nerve grafts along with exogenous delivery of compound was significantly better than the initially developed decellularized grafts, and regeneration was comparable to unprocessed (fresh) nerve graft. There is a potential for clinical translation of these promising results to improve the lives of patients with nerve injuries.

TABLE OF CONTENTS

LIST OF ILLUSTRATIONS

LIST OF TABLES

CHAPTER 1

INTRODUCTION

1.1 The Peripheral Nerve

The Peripheral Nervous System (PNS) consists of nerves and ganglia that connect limbs and organs with the brain and spinal cord which form the Central Nervous System (CNS). Peripheral nerves are made up of axons that communicate through electrical conduction with their target tissues, and transport materials to and from the neuronal soma (cell body). Also contained within the peripheral nerves are Schwann cells that wrap around axons to form an insulating myelin sheath and provide growth factors and structural support. The peripheral nerve is formed by well organized connective tissues that ensheath peripheral axons. The fascial structure of peripheral nerve can be divided into endoneurium, perineurium and epineurium. Endoneurium surrounds axons along with their partner Schwann cells. Perineurium forms a protective sheath around fascicles of endoneurium. Epineurium forms the outermost protective layer which bundles multiple fascicles and blood vessels (Thomas, 1963; Buttermore et al., 2013; King, 2013). A schematic representation of the peripheral nerve is shown in Figure 1.1.

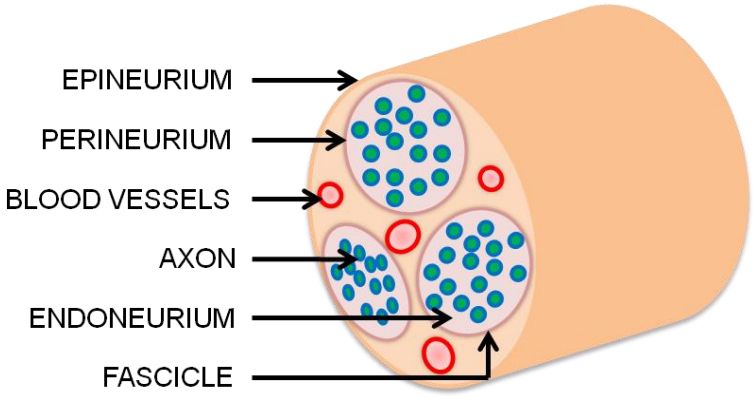

Figure 1.1 Anatomy of the peripheral nerve showing epineurium, perineurium, endoneurium, fascicle, axons and blood vessels.

1.1.1 Peripheral Nerve Injury

Peripheral nerve injuries are relatively common. PNS injuries are estimated to occur in approximately 2.8% of all traumatic injuries, many of which lead to lifelong disabilities. Injuries to the PNS can be caused by accidents, chronic compression, tumor excision, radiation induced injury and birth related defects (Noble et al., 1998; Belkas et al., 2004; Burnett and Zager, 2004). When nerves are subjected to injury, axons in the distal nerve segments undergo a series of well orchestrated events know as Wallerian degeneration. Degenerating axons trigger a cascade of signals leading to non-neuronal cellular responses that eliminate inhibitory debris and molecules and provide a growth permissive environment for regenerating axons (Tofaris et al., 2002; Coleman and Freeman, 2010; Gaudet et al., 2011).

Seddon (Seddon, 1943) classified nerve injuries into neurapraxia, axonotmesis and neurotmesis. Among all the injuries, neurapraxia is the mildest form, where there is no structural damage to the nerve, but there is transient functional loss due to myelin loss and local conduction block. Common causes include compression injuries, with complete recovery of function. Axonotmesis occurs when the axons and myelin sheath are severed, but the surrounding support structures (including perineurium and epineurium) are left intact. Upon axonotmesis, the distal segment of the axon along with myelin undergoes degeneration, causing denervation of end organs. Since the axonal regeneration path is maintained by the undamaged support structures, there are high chances of recovery. Some common causes include severe contusion or crush injury to the nerves. Neurotmesis is the most severe form of injury, where the whole nerve is severed leading to disconnection. It leads to complete loss of function and requires surgical interventions. Sunderland (Sunderland, 1951) further classified the nerve injuries into first-degree, second-degree, third-degree, fourth-degree and fifth-degree.

Sunderland's first-degree is Seddon's neurapraxia and the second-degree is axonotmesis. The third-degree injury occurs when there is axonotmesis along with partial injury to the endoneurium. Recovery of function depends on the magnitude of damage to the

endoneurium. The fourth-degree injury occurs when everything except the epineurium is disrupted, requiring surgical interventions. The fifth-degree injury is equivalent to Seddon's neurotmesis (Seddon, 1943; Sunderland, 1951, 1990; Burnett and Zager, 2004; Campbell, 2008). Figure 1.2 illustrates Seddon and Sunderland classification of nerve injury and shows the relationship between the chances of spontaneous recovery with respect to the extent of tissue damage (Burnett and Zager, 2004). The chance of spontaneous functional recovery decreases with significant tissue damage.

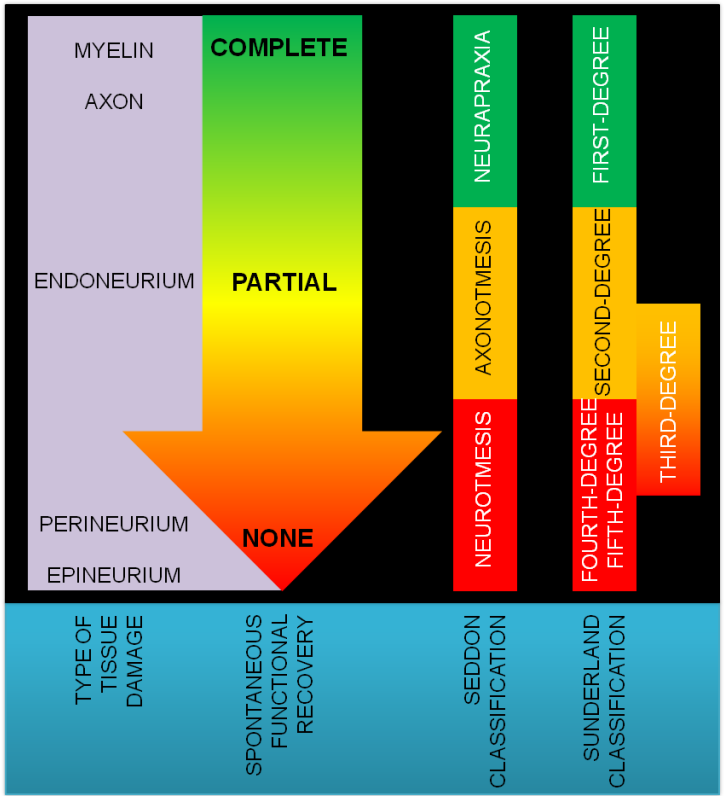

Figure 1.2 Illustration of Seddon and Sunderland grading system for classification of PNS injury.

1.1.2 Long gap Peripheral Nerve Injury: Current treatment

The peripheral nervous system has an inherent capacity to regenerate after injury, but severe injuries (long gap) often lead to very poor and unsatisfactory outcomes (Burnett and Zager, 2004; Szynkaruk et al., 2013). Nerve transection (neurotmesis or Sunderland's 5th degree injury) is the most severe injury to the nerve, which divides the nerve into proximal and

distal stumps. Complete functional recovery after nerve transection is not achieved even with optimal surgical reconstruction (Evans, 2001). In humans, if the inter-stump gap after nerve transection is less than 2 cm (short gap injury), moderate recovery is observed upon nerve repair. For gaps between 2 and 4 cm, the recovery is poor upon reconstruction. For nerve injuries resulting in gaps greater than 4 cm, the chance of achieving functional recovery is very poor to non-existent even after surgical reconstruction (long gap injury) (Reyes et al., 2005; Navarro et al., 2007). Autologous nerve grafts (autografts) are the surgeon's primary choice of treatment, making it the "gold standard" for repair of long gap nerve defects. Allogeneic nerve grafts (allografts) are a known substitute to autografts. Allografts from cadavers are readily available and they contain cellular and microstructural components of a nerve similar to that of autografts (Mackinnon et al., 1987; Midha et al., 1993). On the other hand, nerve conduits and decellularized nerve grafts have been studied to guide axons towards their distal targets for functional reinnervation, but they are limited to short gap injuries.

1.1.3 Need for Alternatives

Autografts are associated with increased risk of infection, inadequate supply, donor-site functional loss and scarring, potential neuroma formation and longer operation times. The major limiting factor with allografts is the requirement of systemic immunosuppressant administration, which predisposes recipients to infection, toxic side effects and other complications (Porayko et al., 1994; Gijtenbeek et al., 1999). Nerve conduits fail to support nerve regeneration across a long gap injury (Moore et al., 2009; Pfister et al., 2011), leaving decellularized nerve grafts as a potential alternative for nerve repair.

1.1.4 Decellularized Nerve Grafts

Due to the limitations cited before with autografts and allografts, there is an increasing interest in decellularized nerve grafts for peripheral nerve repair. The advantage of decellularized nerve grafts over conduits is the presence of intact basal lamina tubes and extracellular matrix proteins that support axonal growth. There are numerous techniques for

preparing decellularized nerve grafts:(1) cold preserved nerve grafts (developed by Mackinnon and colleagues); (2) freezing and freeze-thaw methods; (3) chemical detergent based protocols and (4) irradiation protocol (Ide et al., 1983; Evans et al., 1998; Haase et al., 2003; Hudson et al., 2004; Szynkaruk et al., 2013). Despite this extensive work, decellularized nerve grafts continue to be limited by poor axon regeneration (~30% of unprocessed nerve grafts), disrupted endoneurial tubes, damaged basal lamina and reduced regeneration distances (Whitlock et al., 2009; Szynkaruk et al., 2013).

1.2 Overview of Research Project

1.2.1 Research Objectives

The long-term objective of this research project was to develop a detergent-free nerve decellularization technique for reconstructing a long gap (35 mm) nerve injury. The primary purpose of using a detergent-free decellularization technique is to avoid the use of chemical detergents for decellularization, which can damage the structural components of the tissues during processing and can be toxic upon implantation if not completely removed (Crapo et al., 2011).

1.2.2 Specific Aims

Specific Aim 1: Develop detergent-free decellularized nerve grafts for long gap peripheral nerve reconstruction. Freshly harvested nerve grafts were processed using detergent-free decellularization technique and evaluated for repairing long gap nerve defects with or without exogenous cells inside the grafts. Detergent-free decellularized nerve grafts were compared with established chemical processed nerve grafts.

Specific Aim 2: Establish a nerve injury model to study the difference in molecular profile between a regenerative (growth, short gap) vs. a non-regenerative (no-growth, long gap) nerve gap. A short gap reconstruction that always regenerates and a long gap reconstruction that never regenerates were compared using RT-PCR techniques at the site of injury.

Specific Aim 3: Develop methods to improve nerve regeneration in detergent-free decellularized nerve grafts. Initiated nerve regeneration across a critical gap using biological compounds in a hollow silicone conduit. Use an optimized detergent-free processing technique to obtain improved detergent-free decellularized nerve grafts. Evaluate drugs to improve decellularized nerve grafts for long gap nerve regeneration.

1.2.3 Innovations

The decellularization technique developed in specific aim 1 is simple and cost effective. The nerve architecture is kept intact using this technique while the process initiates events that clear cellular debris. The nerve grafts obtained using this protocol support functional nerve regeneration across a 35 mm gap in a rodent model, which is beyond the critical length. The decellularized nerve graft can be potentially beneficial in the clinical setting, as it does not require the use of harmful chemicals and supports regeneration across a long gap injury.

The growth vs. no-growth model described in specific aim 2 is crucial for better understanding the molecular events occurring at the site of injury. Differential regulation of genes was determined to allow careful selection of compounds that can be used for initiating nerve regeneration across critical nerve defects.

The improved detergent-free decellularized nerve grafts evaluated in specific aim 3 showed improved nerve regeneration compared to a clinically available detergent processed alternative. With the addition of selected drugs, the nerve recovery could be further improved.

1.2.4 Outcome of Research

The successful outcome of the research project will provide an off-the shelf alternative to the clinical gold standard (unprocessed nerve graft) for the treatment of peripheral nerve injuries. The safe, simple and cost effective processing technique can be translated for clinical use, which can improve the quality of life for patients suffering from peripheral nerve injuries.

CHAPTER 2

DETERGENT-FREE DECELLULARIZED NERVE GRAFTS

2.1 Introduction

Injuries to the peripheral nerves are a very common problem for society, leaving patients with lifelong disabilities (Belkas et al., 2004). Even though the peripheral nerves possess an inherent capacity to regenerate upon injury, treatment outcome is often unsatisfactory with severe injuries that lead to long gap defects measuring >3 cm (Burnett and Zager, 2004; Navarro et al., 2007). Autografts have been the primary choice for treatment of nerve gaps, but the associated limitations such as infection risk, inadequate supply and donor-site morbidity have led to exploration of alternative treatment strategies (Ehretsman et al., 1999; Battiston et al., 2005; Santosa et al., 2013) .

Allografts have been implemented in clinical settings as an alternative for autografts as they are readily available and possess cellular and structural components similar to that of autografts (Rivlin et al., 2010). However, the use of allografts necessitates administration of systemic immunosuppressants, which predispose the patients to risks of infection, toxicity, malignancy and other complications (Whitlock et al., 2009; Boyd et al., 2011).

Nerve conduits have been fabricated and evaluated with a variety of materials, but artificial conduits have not been successful for nerve regeneration beyond 3 cm (Whitlock et al., 2009).

Due to the limitations of autografts, allografts and nerve conduits, the search for alternative repair strategies has led to an increasing interest towards developing decellularized nerve grafts for repair of peripheral nerve injuries (Rivlin et al., 2010; Boyd et al., 2011; Szynkaruk et al., 2013). Components of decellularized nerve grafts such as basal lamina and extracellular matrix proteins support regenerating axons (Hudson et al., 2004; Nagao et al.,

2011). Some of the commonly used decellularization techniques include (1) cold preservation, (2) chemical detergent based decellularization, (3) freeze-thawing and (4) irradiation. These grafts have found limited use for repairing long gap nerve defects due to associated limitations such as damaged basal lamina, disrupted endoneurial tubes, limited regeneration distance and poor axonal regeneration (Hudson et al., 2004; Whitlock et al., 2009; Szynkaruk et al., 2013).

The specific aim of this work is to develop a detergent-free decellularization technique for repairing long gap peripheral nerve injuries in a rodent model. The detergent-free processing technique was developed to initiate Wallerian degeneration *in vitro,* as this process is responsible for clearing myelin debris and other inhibitory components in the distal nerve segment after injury. During Wallerian degeneration, Schwann cells de-differentiate and initiate a cascade of events to phagocytose debris and recruit macrophages to aid in effective clearance (Abercrombie and Johnson, 1946; Stoll et al., 1989; Griffin et al., 1992; Brück, 1997). It has been shown that Schwann cells are capable of performing phagocytosis in culture (Reichert et al., 1994), a function we leveraged to our favor in this work. After *in vitro* Wallerian degeneration has occurred, the nutrient supply to the cells inside the nerves is withdrawn to decellularize the nerves. The decellularized nerve grafts yielded by the detergent-free processing technique was evaluated for nerve regeneration across a 35 mm long defect. We also conducted experiments with exogenous cells seeded throughout the length of the detergent-free decellularized grafts and established chemical detergent processed nerve grafts.

2.2 Experimental Section

All animal procedures were performed as per approved Institutional Animal Care and Use Committee (IACUC) protocols at the University of Texas Southwestern Medical Center at Dallas, Texas. Rats were anesthetized using intraperitoneal (IP) injection of a drug cocktail containing ketamine hydrochloride (75 mg/kg) and dexmeditomidine hydrochloride (0.5 mg/kg). Following terminal experiments, rats were euthanized using IP injection of sodium pentobarbital (120 mg/kg). Subcutaneous injection of buprenorphine (Buprenex) and chewable tablets of carprofen (Rimadyl) were placed in the cage for post-operative pain care.

2.2.1 Sciatic Nerve Harvest

Rats were anesthetized and both hind limbs were shaved and sterilized by application of alcohol prep pads and betadine three times. Sciatic nerves were harvested from both hind limbs of thirty nine donor rats (Lewis, male, >350 g; Charles River) under aseptic conditions. Briefly, the skin was incised using a scalpel, and the underlying sciatic nerve was exposed using thigh muscle-splitting procedure. The entire length of the sciatic nerve from greater sciatic foramen to the distal trifurcation was carefully dissected and harvested, yielding approximately 4.2 cm long nerves. Nerves were handled in aseptic conditions for further processing.

2.2.2 Schwann Cell Culture

Cultivation of Schwann cells for this study was performed as described elsewhere (Komiyama et al., 2003). Briefly, sciatic nerves of rats (male, Lewis) were harvested and washed in phosphate-buffer saline (PBS; Gibco, USA). 1 mm segments of nerve were digested with 0.05% collagenase/dispase in 10 ml Boehringer Mannheim medium (Boehringer Mannheim, Germany), followed by trituration and incubation for 3h in a cell culture incubator at 37 °C, 5% CO_2. To inactivate the digestion mixture, 10 ml of medium containing 10% fetal bovine serum (FBS; Hyclone, USA) was added and the nerves were subjected to mechanical dissociation. Further, the nerve fragments were plated onto a T75 flask coated with poly-L-

lysine (0.1%) and cultured using Schwann cell medium containing 2.5% FBS. Purified Schwann cells were used to evaluate the effects of exogenous cell supplemented decellularized grafts.

2.2.3 Skin Derived Progenitor Cell Culture

Skin derived progenitor (SKPs) cells were cultured as per published protocols (Toma et al., 2001; Fernandes et al., 2004). Briefly, dorsal skin from adult rats (Lewis, male) was dissected and minced into 2-3 mm^2 pieces under aseptic conditions. Tissues were subjected to enzymatic digestion using 0.1% trypsin for 45 min in a cell culture incubator at 37 °C, 5% CO_2, and dissociated mechanically before passing the cells through a 40 µm cell strainer to remove larger clumps. Cells were cultured in DMEM-F12 medium (Invitrogen, USA) containing FGF2 (40 ng/ml) and EGF (20 ng/ml) (both from Peprotech, USA) using T25 flasks in cell culture incubator. SKPs were mechanically dissociated and passaged and cultured in medium containing 75% fresh medium and 25% conditioned medium from the initial flask. Purified SKPs were used to evaluate the effects of decellularized grafts supplemented with exogenous cells.

2.2.4 Detergent-free Decellularization

Detergent-free decellularized nerve grafts (Decell) were obtained using a protocol developed in our laboratory. Freshly harvested sciatic nerves from donor rats were rinsed in Dulbecco's Modified Eagle Medium (DMEM; Gibco, USA) containing 10% FBS and 4% penicillin/streptomycin/amphotericin B (Antibiotic-Antimycotic; Gibco, USA). After rinsing, the nerves were sutured (10-0 nylon; Arosurgical, USA) onto sterile rubber holders (5 x 1 x 1 cm) to retain nerve length for processing.

For initiating Wallerian degeneration *in vitro*, nerves along with rubber holders were transferred into 15 ml conical tubes containing 7 ml DMEM10 medium (DMEM10 = Dulbecco's Modified Eagle Medium with 10% FBS and 2% penicillin/streptomycin/amphotericin B) and agitated for 2 weeks inside a cell culture incubator kept at 37°C with 5% CO_2. During the culture period, 3 ml of DMEM10 from the tubes were replaced with 3.5 ml of fresh DMEM10 every 3 days to replenish nutrients in the medium.

To decellularize the nerves, DMEM10 medium from the tubes were replaced with PBS containing 2% penicillin/streptomycin/amphotericin B and agitated for 1 week at 37 °C, 5% CO_2 in a cell culture incubator. This process was used to abruptly withdraw nutrient supply to the grafts and to remove debris by constant agitation. Processed grafts were stored at 4 °C until implantation. Figure 2.1 demonstrates the process used for preparing Decell grafts for implantation.

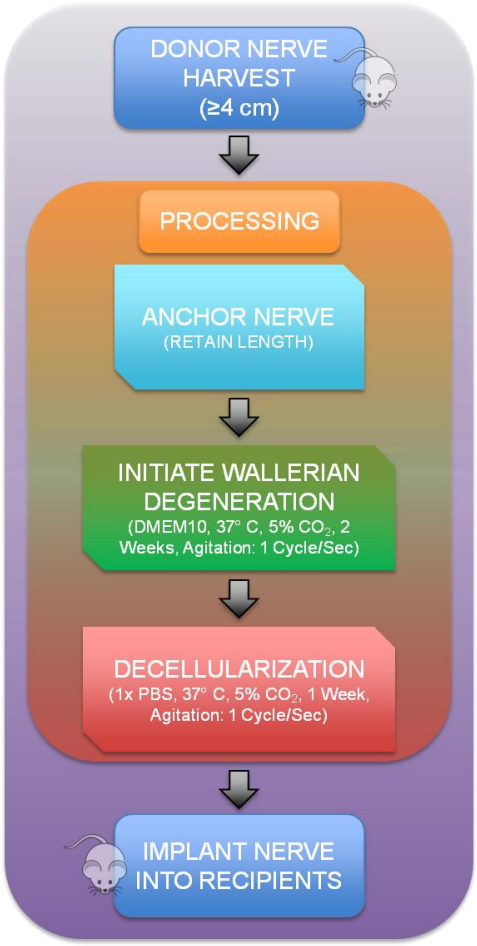

Figure 2.1 Decell graft processing and implantation overview

2.2.5 Immunohistochemical Analysis of Decell Grafts

For immunohistochemical (IHC) purposes, samples of Decell grafts were immersion fixed in 4% paraformaldehyde (Sigma Aldrich, USA) overnight and washed in PBS. Samples were prepared for cryosectioning, and embedded into OCT blocks. 10 µm sections were blocked using 4% goat serum (Life Technologies, USA) and stained with mouse anti-laminin B2 gamma 1 (D18) primary antibody (Abcam, ab80581, 1:300), and goat anti-mouse Alexa Fluor 488 secondary antibody (Molecular Probes, A11017, 1:300).

2.2.6 Ultra-Structural Analysis Using TEM

For high magnification imaging of myelin and cellular components, Decell nerves were immersion fixed in 3% glutaraldehyde (Sigma Aldrich, USA). Samples were processed for transmission electron microscopy (TEM) as described elsewhere (Mackinnon et al., 1982). Briefly, nerves were post-fixed in osmium tetroxide and embedded in Araldite 502. Ultra-thin sections were cut and stained with uranyl acetate-lead citrate solution.

2.2.7 Exogenous Cell Loaded Decell Grafts

Schwann cell loaded Decell grafts (Decell + SC) were prepared by injecting 10^6 cells in culture medium into the grafts before implantation. Similarly, SKPs loaded Decell grafts (Decell + SKPs) were prepared by injecting 10^6 cells into the grafts before implantation.

2.2.8 Detergent Decellularized Nerve Grafts

Detergent decellularized nerve grafts (Detergent Decell) were processed by decellularization and elimination of chondroitin sulfate proteoglycans (CSPG) using established protocols (Hudson et al., 2004; Neubauer et al., 2007). Freshly harvested sciatic nerves were placed in RPMI 1640 medium (Gibco, USA) to clear connective and fatty tissues. As described before, nerves were secured onto rubber holders using 10-0 nylon sutures for retaining length during processing.

Decellularization of nerves was achieved by transferring the nerves into 15 ml conical tubes containing double distilled water (DD; 18 MΩ) at 25 °C for 7 hr under constant agitation.

Table 2.1 describes the formulations of solutions used for detergent-decellularization. All the reagents were purchased from Sigma Aldrich, USA unless specified. After DD water wash, nerves were transferred into 15 ml conical tubes containing SB-10 buffer, and were subjected to constant agitation at 25 °C for 15 hr. Nerves were rinsed with washing buffer for 15 min. The washing buffer was replaced with SB-16 buffer and again agitated at 25 °C for 24 hr followed by rinsing in washing buffer 3 times for 5 min each. Nerves were then transferred into new 15 ml tubes containing SB-10 buffer and agitated at 25 °C for 7 hr followed by rinsing with washing buffer for 15 min. The washing buffer was replaced with SB-16 buffer and agitated at 25 °C for 15 hr, followed by three washes with 10 mM phosphate-50 mM sodium buffer for 15 min each.

Table 2.1 Formulations used for preparing buffers and detergent solutions

	Solutions	Formulations
1	10 mM Phosphate - 50 mM Sodium buffer	NaCl 1.860g $NaH_2PO_4.H_2O$ 0.262g $NaH_2PO_4.7H_2O$ 2.170g Add DD water to 1 L
2	50 mM Phosphate - 100 mM Sodium buffer (Wash buffer)	NaCl 0.560g $NaH_2PO_4.H_2O$ 1.310g $NaH_2PO_4.7H_2O$ 10.850g Add DD water to 1 L
3	SB-10 solution	Sulfobetaine-10 125 mM 10 mM Phosphate - 50 mM Sodium buffer
4	SB-16 solution	Sulfobetaine-16 0.6 mM Triton X-200 0.14% 10 mM Phosphate - 50 mM Sodium buffer

Following detergent processing, inhibitory CSPGs were eliminated using Chondroitinase ABC (ChABC) treatment. Detergent-processed nerves were incubated in PBS containing 2 units/ml ChABC at 37°C and 5% CO_2 for 16 h in a cell culture incubator. The process was completed by washing the nerves using cold Ringer's solution 3 times for 15 min each and Detergent Decell grafts were stored in Ringer's solution at 4 °C until implantation.

2.2.9 Implantation of Nerve Grafts

Recipient rats were prepared under aseptic conditions as described previously using alcohol prep pads and betadine. All groups received 35 mm long nerve grafts in reversed orientation across transected right sciatic nerve at mid-thigh level. Unprocessed nerve grafts were implanted immediately after harvest from donor rats under aseptic conditions. The entire length of sciatic nerve grafts was accommodated as described in our previous work(Vasudevan et al., 2013). Briefly, constructs were placed around the anterior head of biceps femoris muscle and coapted to proximal and distal stumps using 10-0 nylon epineurial sutures under an operating microscope. Figure 2.2b illustrates the implantation procedure for nerve grafts.

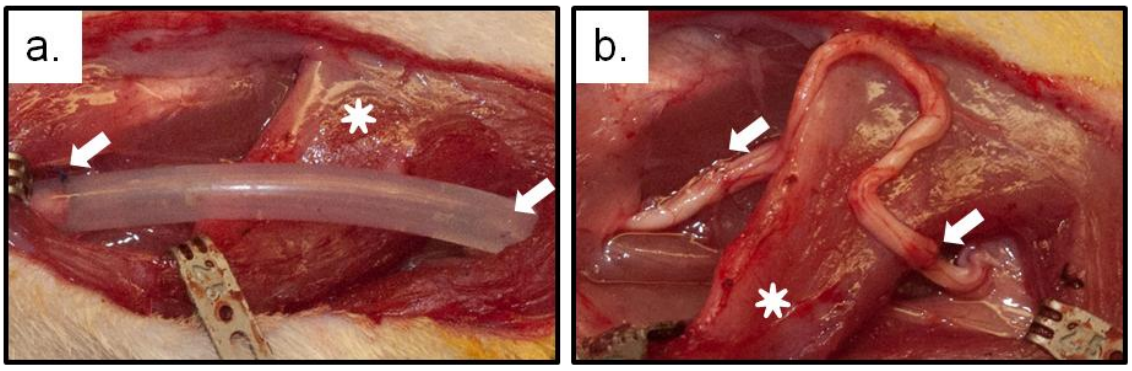

Figure 2.2 Intraoperative images showing implantation of long conduits and nerve grafts. (a) 3.5 cm silicone tube, and (b) 3.5 cm nerve graft. Silicone tube conduits and nerve grafts were looped around the anterior head of biceps femoris muscle (*). Arrows indicate coaptation sites. Proximal nerve stump is on the left side of the images (Vasudevan et al., 2013)

Silicone conduits were implanted by inserting the proximal and distal ends of the sciatic nerve into the lumen of the conduit, which was placed around the biceps femoris muscle as shown in Figure 2.2a.

2.2.10 Experimental Setup

Sixty four rats (male, Lewis, 250 - 300g) were randomly assigned into six groups: (1) Unprocessed nerve graft (positive control, n=6 per time point), (2) Detergent-free decellularized grafts (Decell, n=6 per time point), (3) Decell loaded with Schwann cells (Decell + SC, n=6 per time point), (4) Decell loaded with SKPs cells (Decell + SKPs, n=6 per time point), (5) Detergent decellularized grafts (Detergent Decell, n=6) and (6) Silicone tube (negative control, 3.5 cm length, 1.6 mm ID, n=6 per time point). All groups other than Detergent Decell group were evaluated at 6 weeks, 8 weeks and 12 weeks post-implantation. Detergent decell group was evaluated only at 12 weeks for comparison purposes. An overview of the experimental evaluation is demonstrated in Figure 2.3.

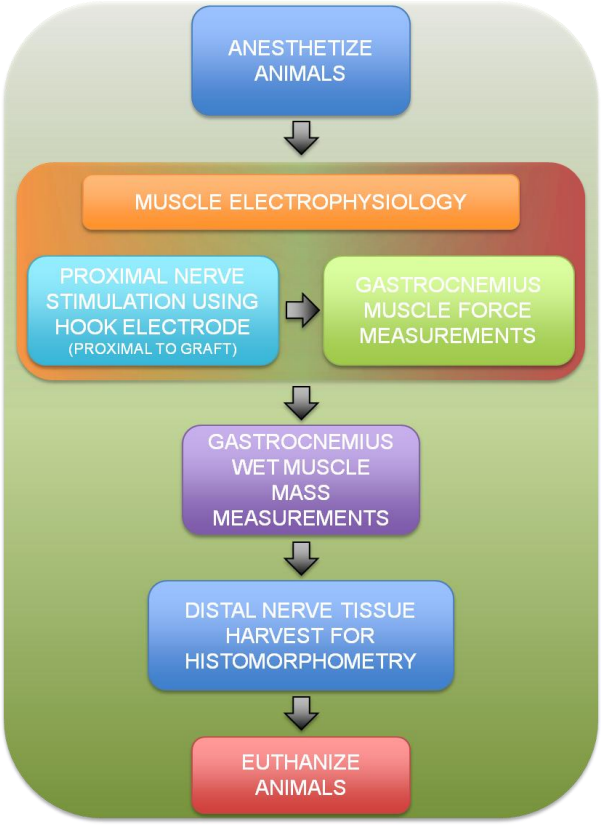

Figure 2.3 Flowchart of experimental procedures for evaluation of nerve regeneration

2.2.11 Gastrocnemius Muscle Electrophysiology

Gastrocnemius muscle specific tetanic tension (maximum tension normalized to muscle weight) was used as a parameter for functional nerve regeneration. At each time point, animals were anesthetized and immobilized in a rigid frame consisting of clamps on the pelvis and a stereotaxic head holder. The gastrocnemius muscle in both experimental and contralateral limbs was exposed followed by excision of soleus and plantaris. The Achilles tendon was isolated with its calcaneal insertion and detached from the remainder of the bone, and a 4-0 nylon suture (Ethicon, USA) was tied to form a loop at the tendon insertion and attached to a strain gauge (Kutile BG1250) along the line of pull for measuring muscle tension. The hind limb to be studied was further stabilized using clamps on the hind foot. Sciatic nerve proximal to the reconstruction was stimulated using bipolar hook electrodes, which were electrically isolated

using cotton soaked in mineral oil. Figure 2.4 shows the setup used for performing muscle electrophysiology.

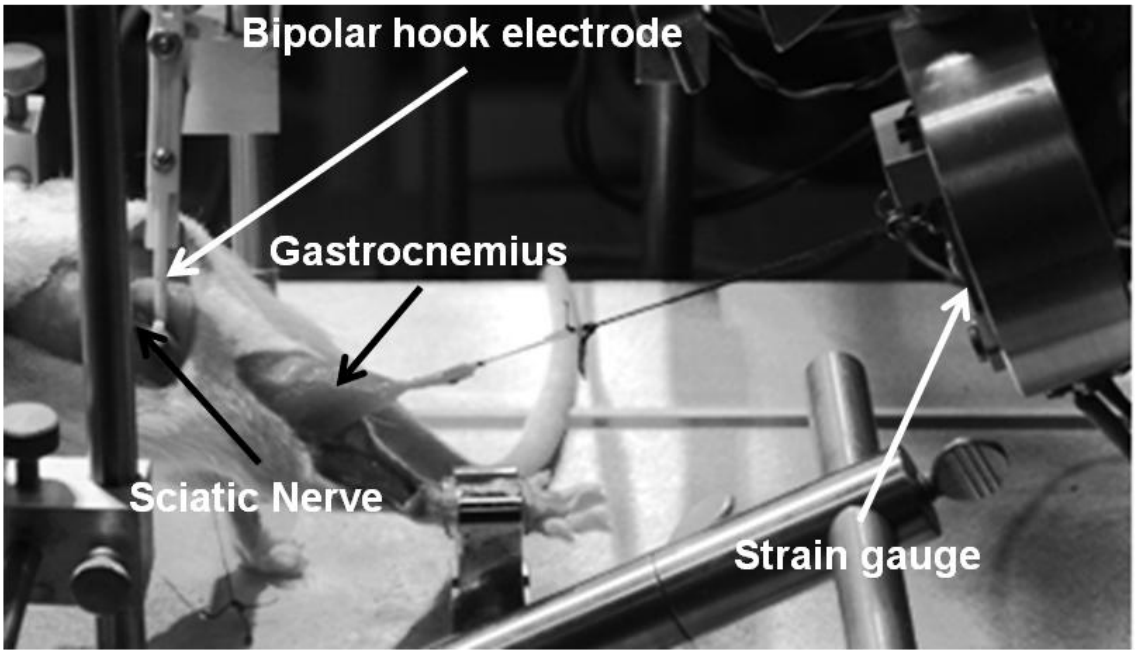

Figure 2.4 Muscle electrophysiology setup used for evaluation of nerve regeneration

To measure tension, the nerve was stimulated with 100 µs square wave pulses with voltage 3X above twitch threshold. Peak twitch tension was obtained by adjusting muscle length and all remaining tension measurements were digitized and recorded at this setting (CED 1404 Plus, Signal 3.0). Peak tetanic tension was determined by stimulating the sciatic nerve with 100 pulses/sec for 600 ms. For comparison of tetanic specific tension between groups, normalized specific tension [(experimental tension per gram)/(contralateral tension per gram)] was determined.

After performing muscle electrophysiology, gastrocnemius muscles from both experimental and contralateral sides were harvested for obtaining wet muscle mass. The ratio of experimental to contralateral muscle mass was used for comparison among groups. Contralateral muscles served as an internal control to adjust for variability between animals.

2.2.12 Evaluation of Nerve Regeneration Using Histomorphometry

For evaluating regeneration across the nerve grafts, semi-automated quantitative histomorphometry was performed on the distal sciatic nerve stump. Nerve stumps were harvested and immersion fixed in 3% glutaraldehyde at 4 °C. Samples were prepared as per established protocols (Hunter et al., 2007). Briefly, nerve tissues were post-fixed in 1% osmium tetroxide, serial dehydration was performed using ethanol and specimens were embedded using Araldite 502 and semithin sections were cut. Sections were stained with 1% toluidine blue and mounted on glass slides for imaging.

Analysis of tissue was performed using Leco IA32 Image Analysis System to obtain total number of axons, myelin width and fiber distribution for comparison among groups. Figure 2.5 shows the steps involved in performing quantitative histomorphometry. Bright field images of multiple fields were analyzed using the system and myelin was covered by pixels by selective thresholding. To remove components other than myelin, selected pixels were trimmed using the slice function and eliminated using the kill function. Following myelin selection, areas surrounded by myelin (axon) were automatically selected by the program. Pixels other than axons were removed by using kill function and the nerve along with myelin was quantified for multiple parameters.

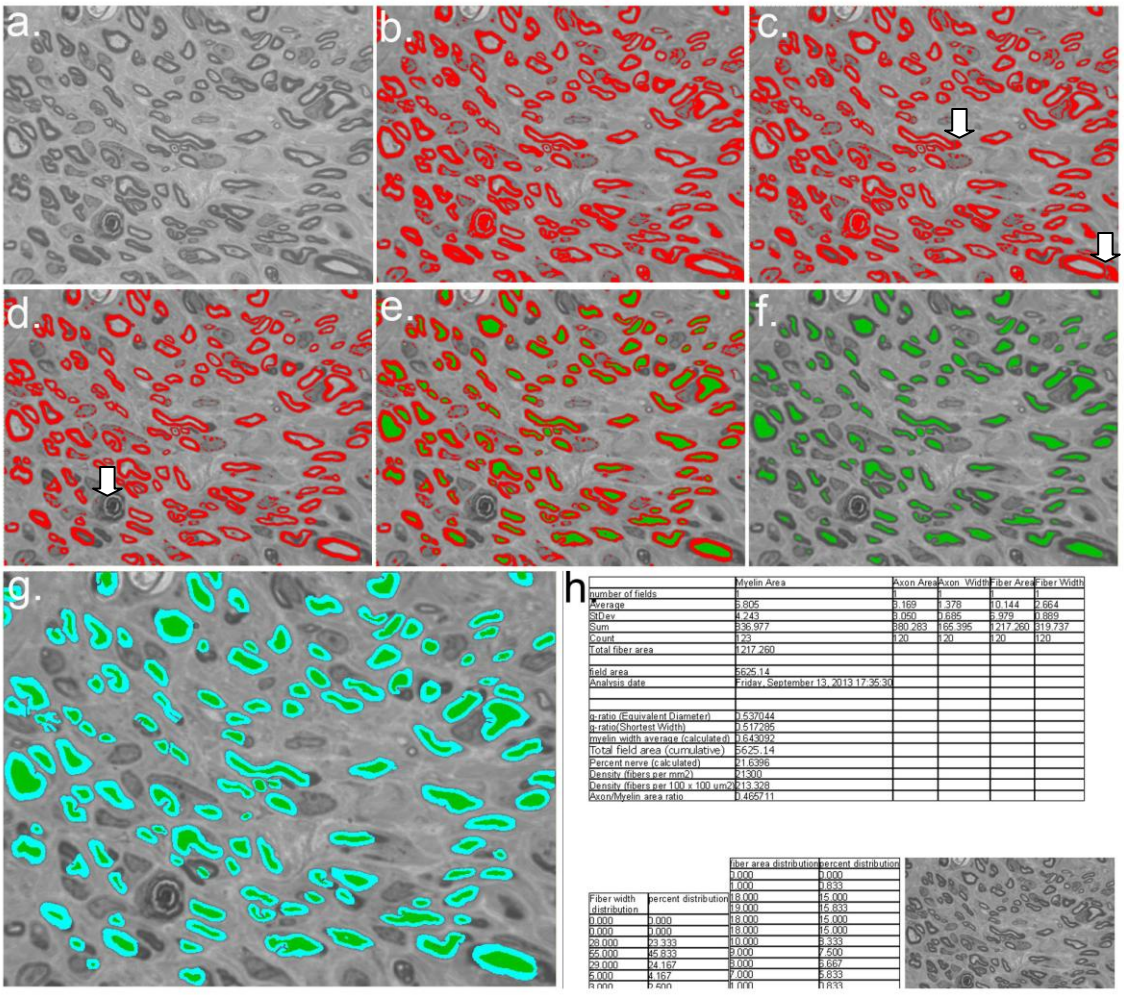

	Myelin Area	Axon Area	Axon. Width	Fiber Area	Fiber Width
number of fields	1	1	1	1	1
Average	6.805	3.169	1.378	10.144	2.664
StDev	4.243	3.050	0.685	5.979	0.889
Sum	836.977	380.283	165.395	1217.260	319.737
Count	123	120	120	120	120
Total fiber area	1217.260				
field area	5625.14				
Analysis date	Friday, September 13, 2013 17:35:30				
g-ratio (Equivalent Diameter)	0.537044				
g-ratio(Shortest Width)	0.517285				
myelin width average (calculated)	0.643092				
Total field area (cumulative)	5625.14				
Percent nerve (calculated)	21.6396				
Density (fibers per mm2)	21300				
Density (fibers per 100 x 100 um2)	213.328				
Axon/Myelin area ratio	0.465711				

Fiber width distribution	percent distribution
0.000	0.000
0.000	0.000
28.000	23.333
55.000	45.833
29.000	24.167
6.000	5.167
3.000	2.500

fiber area distribution	percent distribution
0.000	0.000
1.000	0.833
18.000	15.000
19.000	15.833
18.000	15.000
18.000	15.000
10.000	8.333
9.000	7.500
8.000	6.667
7.000	5.833
1.000	0.833

Figure 2.5 Histomorphometry analysis on regenerated nerves. (a) Selected field showing regenerated axons. (b) Selection of myelin by carefully performing threshold. (c) Slicing unwanted regions of the myelin (arrow) and debris. (d) Eliminating regions other than myelinated axons using kill option (arrow). (e) Analyzing field to obtain axons (green) and myelin (red). (f) Eliminating pixels other than axons. (g) Analyzing only myelinated axons in the field. (h) Sample of the report showing details of the analyzed field.

2.2.13 Statistical Data Analysis

The results were analyzed using Student's t-test between groups with significance at $P<0.05$. Multiple groups were compared using one-way analysis of variance (ANOVA) with $P<0.05$ and Newman-Keuls Post-hoc method was used for pairwise comparison (Statistica 4.5). Data is presented in terms of mean ± standard deviation (SD).

2.3 Results and Discussion

2.3.1 Decell Grafts Characterization

Decell grafts were stained with antibodies against laminin to observe endoneurial tubes. After the 3 week long processing, endoneurial tubes were preserved as shown in Figure 2.6. The longitudinal sections show continuity of basal lamina, which is essential for guiding regenerating axons to the distal targets. The process preserves the endoneurial structure which facilitates regeneration.

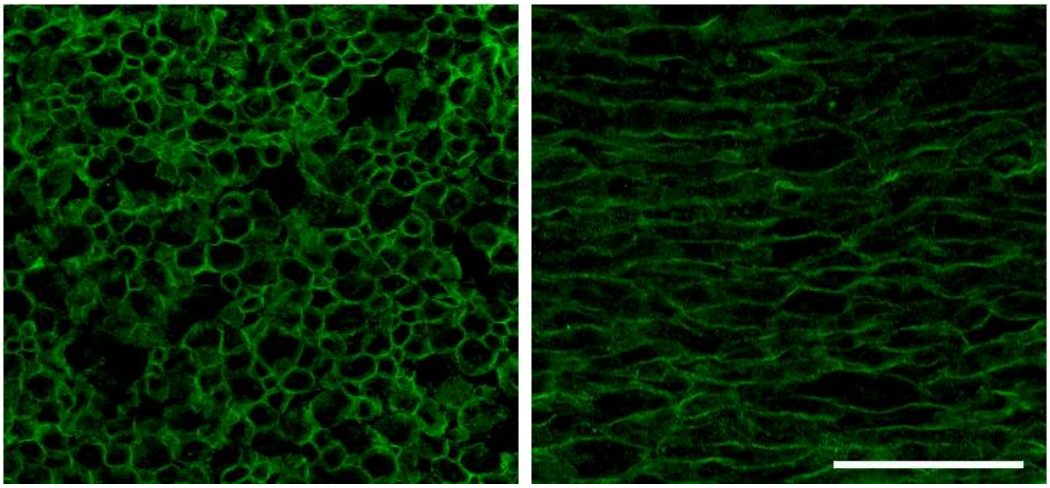

Figure 2.6 Laminin staining of Decell grafts to visualize endoneurial tubes. Cross-sections (left) and longitudinal section (right) showing preserved endoneurial microstructure. Scale bar 100 µm.

To compare the effects of *in vitro* Wallerian degeneration and decellularization on myelin and cellular components of the nerve, we subjected nerves to detergent-free decellularization technique developed by our lab and compared these with nerves that were

immersed in PBS for 3 weeks as a control. Myelin sheaths in the Decell grafts had disintegrated to a loose structure, but the control group treated with PBS retained compact myelin as seen in Figure 2.7. Schwann cells in the nerve have the potential to perform cell-mediated myelin degradation (Reichert et al., 1994), and this was used to our advantage by keeping the cells in the nerve supplemented with DMEM10 medium. The *in vitro* initiation of Wallerian degeneration helps in clearance of cellular debris and inhibitory myelin. Detergent-free decellularization technique can be used to process grafts which readily integrated upon implantation to form a supportive environment for regenerating axons.

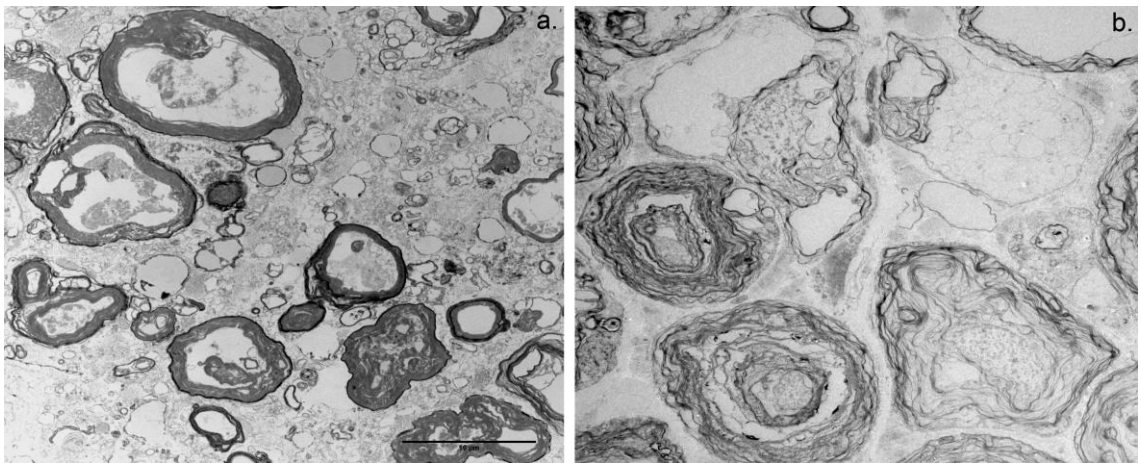

Figure 2.7 TEM images of nerve grafts treated with PBS only for 3 weeks (left) and Decell grafts (right). Scale bar 10 µm.

2.3.2 Schwann Cell and SKPs Cell Culture

Schwann cells play an important role in nerve regeneration by providing support to regenerating axons (Dowsing et al., 1999). To study the effects of Schwann cell supplementation of the detergent-free processed grafts, we successfully cultured primary Schwann cells and characterized them with S-100 antibody (Figure 2.8). These cells were injected into Decell grafts to obtain Decell + SC grafts which were implanted to reconstruct a long gap nerve injury.

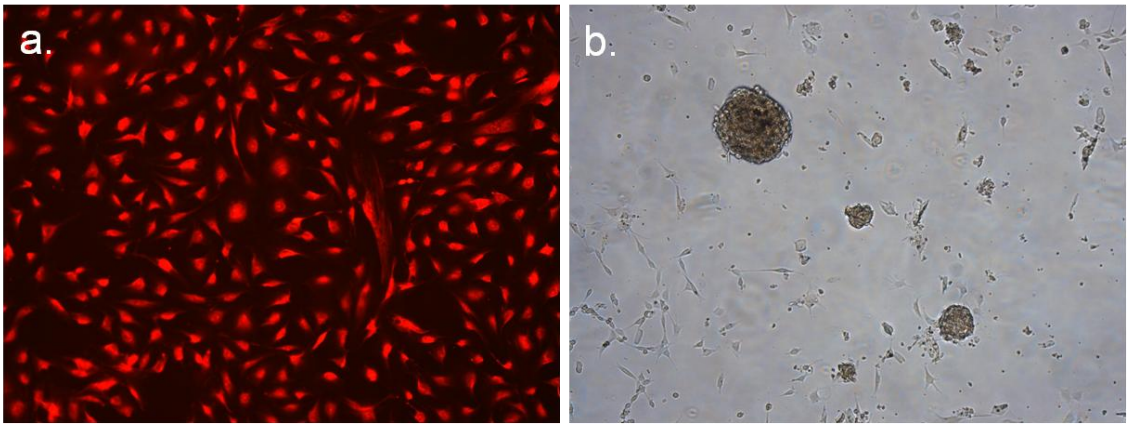

Figure 2.8 (a) Cultured Schwann cells stained for S-100. (b) SKPs spheres in culture

Skin derived progenitors (SKPs), a population of cells known to have the capacity to differentiate to Schwann cells to aid PNS regeneration (Lu et al., 2012), were used to supplement detergent-free processed nerve grafts. We were successful at culturing these cells from adult rat tissues (Figure 2.8) and injected them along the length of a Decell graft forming Decell + SKPs grafts. These grafts were implanted to reconstruct a long gap injury, to study the effect of undifferentiated SKPs on nerve regeneration.

2.3.3 Recovery of Gastrocnemius Muscle Function

Regeneration across nerve grafts was studied at 6 weeks, 8 weeks and 12 weeks post-implantation. Time points were chosen to estimate the optimum time required for functional nerve regeneration using decellularized nerve grafts to reconstruct long nerve gaps.

All the groups, including unprocessed nerve graft did not show recovery of muscle function at the 6 week time point. We determined that the time required for regeneration and formation of functional synapses is longer than 6 weeks using this model.

Animals evaluated at the 8 week time point showed recovery of muscle function in groups implanted with Unprocessed nerve graft and Decell + SC grafts. All the other groups did not show signs of muscle recovery during the 8 week implantation period. The tetanic specific tension and wet muscle mass comparison between Unprocessed nerve graft group and Decell + SC group is shown in Figure 2.9. Unprocessed nerve grafts contain native cellular and

structural components and are considered to be a gold standard for nerve repair. The Decell + SC group had Schwann cells re-seeded within the nerve matrix to partially simulate an unprocessed nerve graft. Although the Unprocessed nerve graft group provides a better regenerative environment, there was no significant difference in terms of tetanic specific tension and wet muscle mass. This implies that the preserved matrix of Decell grafts along with cellular support from Schwann cells is sufficient to promote functional recovery of target muscle.

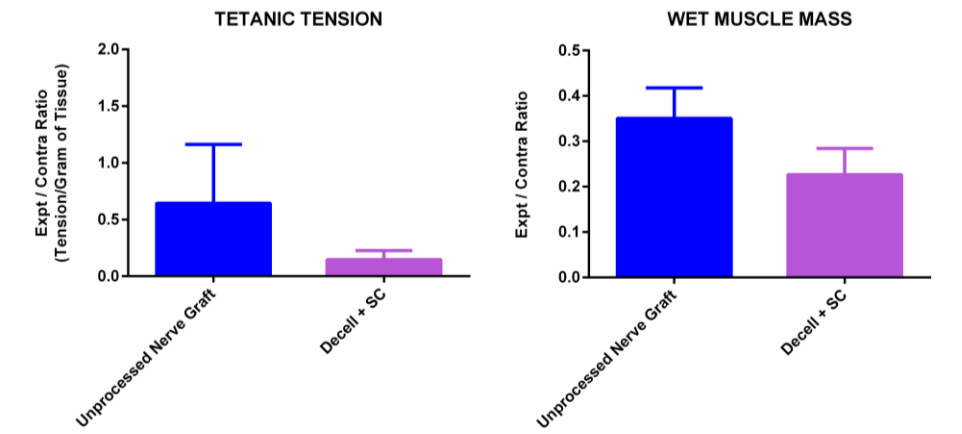

Figure 2.9 Functional recovery of gastrocnemius muscle at 8 weeks post-implantation. Graphs show tetanic specific tension and wet muscle mass between Unprocessed nerve graft and Decell + SC groups.

Evaluation of muscle recovery at 12 week time point showed that the Unprocessed nerve graft group and Decell group had function (Figure 2.10). The Decell + SC group showed degeneration at the distal grafts in some cases, and did not have any function at this time point. Decell + SKPs, Detergent Decell and Silicone tube group did not have muscle function. It was interesting that the supplementation of Schwann cells within Decell grafts accelerated regeneration to form functional connection with the target muscle at 8 weeks, but did not exhibit function at the 12 week time point.

There was no significant difference between the functionally regenerated Unprocessed nerve graft and Decell groups in terms of tetanic specific tension, but the muscle mass comparison showed higher muscle mass in the Unprocessed nerve graft group. The

Unprocessed nerve graft group also had earlier functional recovery as shown at the 8 week time point, which would be a reason for superior muscle mass. However, we found that the Decell group without addition of external factors was sufficient to promote functional regeneration, comparable to the Unprocessed nerve graft group in this long nerve gap model.

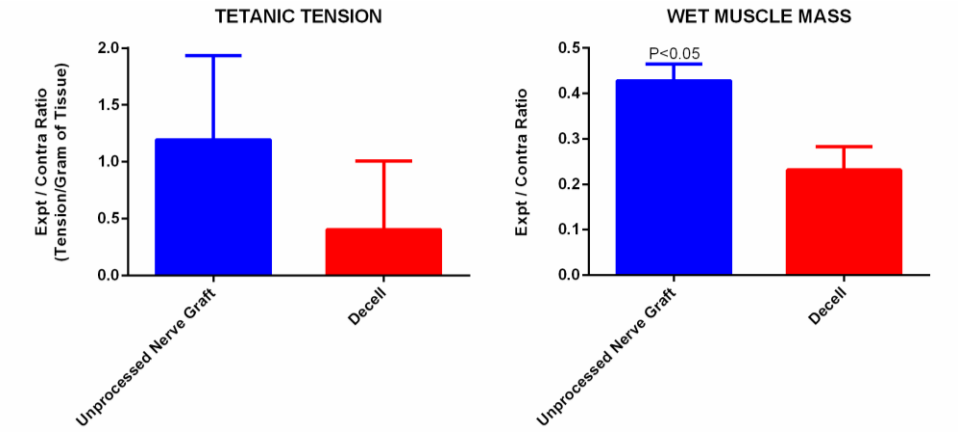

Figure 2.10 Gastrocnemius muscle functional recovery at 12 weeks post-implantation. Tetanic specific tension and wet muscle mass comparison between Unprocessed nerve graft and Decell groups.

2.3.4 Nerve Regeneration Analysis Using Quantitative Histomorphometry

Myelinated axons in the distal nerve stumps were used as a measure to evaluate nerve regeneration in all groups. Total number of axons, myelin width and fiber distribution (according to thickness) were obtained using quantitative histomorphometry.

Even though there was no recovery of muscle function at the 6 week time point, we observed axon regeneration in the distal nerve stumps of Unprocessed nerve graft group only. Other groups did not show signs of regeneration. This time point was too early to study regeneration across a 35 mm long gap injury using processed nerve grafts.

Myelinated axons regenerated across the long gap into the distal nerve stumps in Unprocessed nerve graft and Decell + SC groups at 8 weeks (Figure 2.11). Other groups did not have myelinated axon growth at this time point. The Decell + SC grafts contained structural and cellular components (Schwann cells) that promoted nerve regeneration across a long gap.

It is promising at this point to use Schwann cell seeded Decell grafts to obtain nerve regeneration as an alternative to autografts.

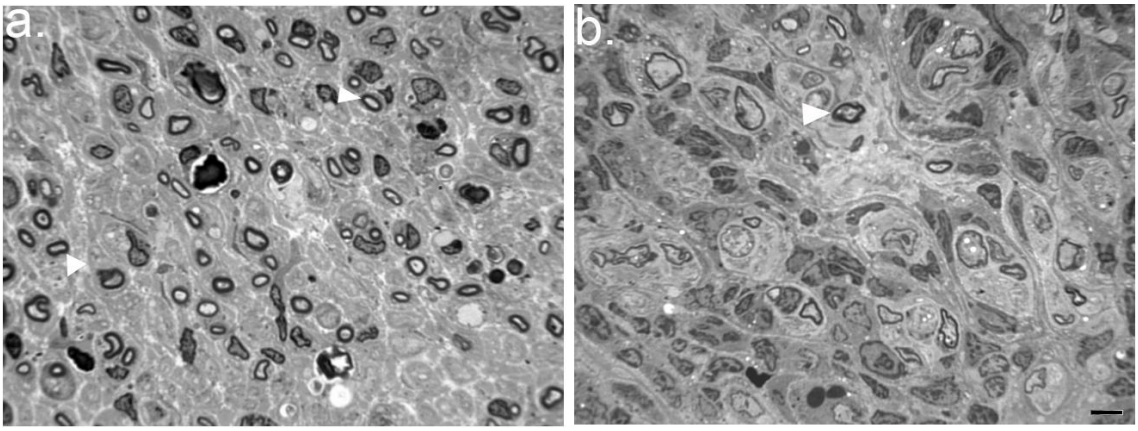

Figure 2.11 Bright field image of toluidine blue stained sections showing regeneration of myelinated axons in the distal nerve stumps at 8 weeks. (a) Unprocessed nerve graft, (b) Decell + SC. Scale bar 5 µm. Arrows showing myelinated axons.

We compared total number of axons and myelin width between the regenerated groups to study the efficacy of Decell + SC grafts compared to Unprocessed nerve grafts (Figure 2.12). Better regeneration is observed in the Unprocessed nerve graft group compared to the Decell + SC group, but there is no significant difference in maturity of myelination as shown by the myelin width data. Unprocessed nerve graft promotes robust regeneration, but the myelination of the Decell + SC group supported comparable muscle function. Presence of larger caliber fibers suggests that the maturity of axons in the Unprocessed nerve graft group was superior to that of Decell + SC group as shown by the fiber distribution data. However, uninjured nerve fiber distribution suggests that both thin and thick fibers contribute to complete function of a matured nerve.

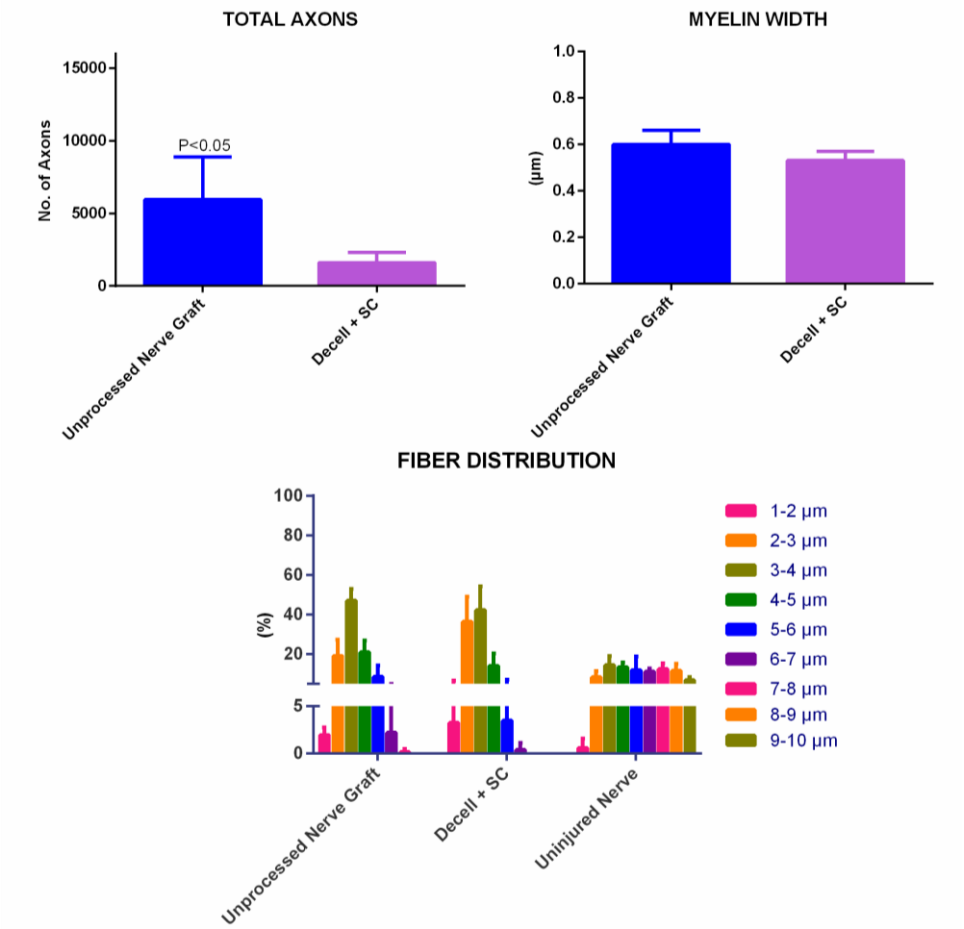

Figure 2.12 Quantification of total axons, myelin width and fiber distribution at 8 weeks. Data compare regeneration of Unprocessed nerve graft, Decell + SC groups and Uninjured Nerve.

Nerve regeneration at the 12 week time point was observed in all the groups other than Decell + SKPs and silicone tube. In the following comparisons, Decell + SKPs and silicone tube groups were omitted entirely because they showed no regeneration. Bright field images of regenerated axons are seen in Figure 2.13, which shows maximum regeneration in the Unprocessed nerve graft group, least in the Decell + SC group, and intermediate in the Decell and Detergent Decell groups.

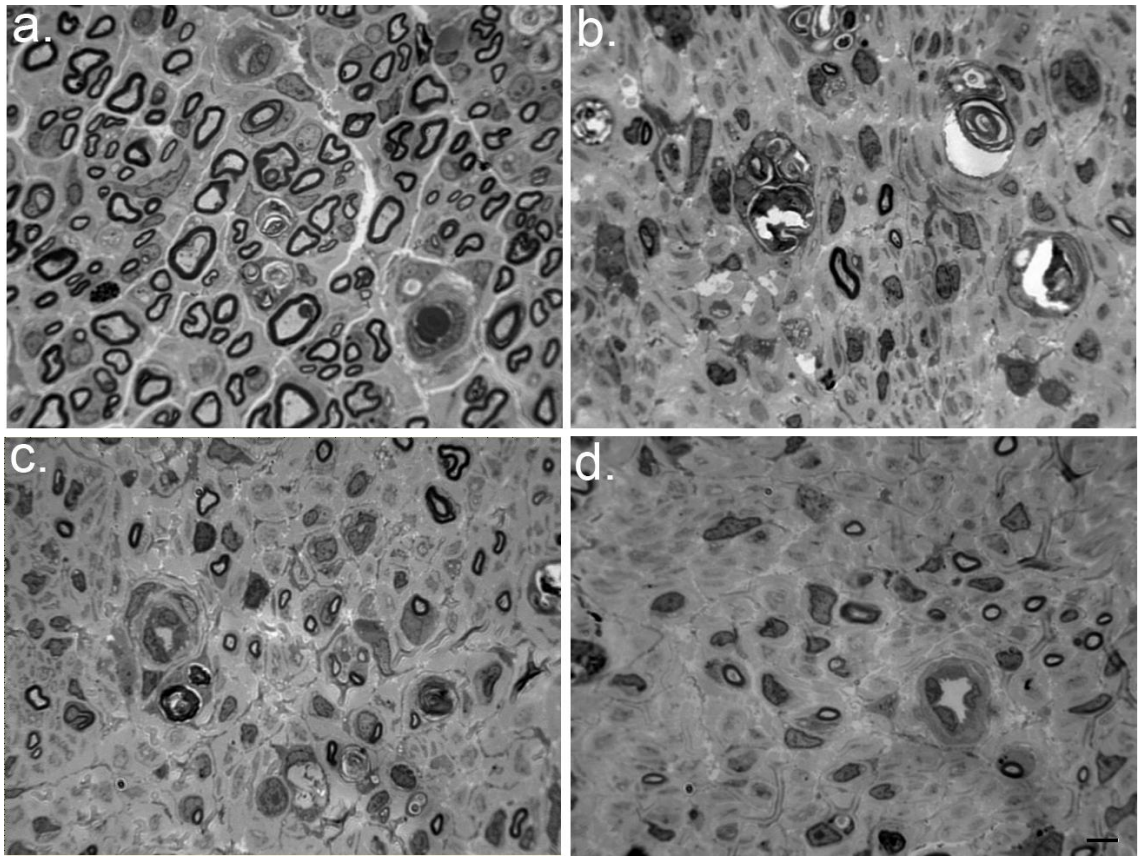

Figure 2.13 Bright field image of distal nerve stumps at 12 weeks post-implantation. Regeneration of myelinated axons can be seen in (a) Unprocessed nerve graft, (b) Decell + SC, (c) Decell, and (d) Detergent Decell group. Scale bar 5 µm

Of the groups that regenerated, the total number of axons in the Unprocessed nerve graft group was significantly higher than other groups, Decell + SC group showed the least amount of axons and the regeneration of axons in Decell and Detergent Decell groups were comparable as shown in Figure 2.14. Importantly, the Decell group regenerated axons and promoted functional muscle recovery without addition of exogenous factors. The Detergent Decell group promoted regeneration across a long gap, which previously had not been tested. The Decell group proved to be superior to the Detergent Decell group due to the recovery of function. This may be due to the absence of chemical detergents during processing of Decell grafts.

Myelin width was used to assess maturity of myelination, which indicated that Unprocessed nerve graft, Decell and Detergent Decell groups have comparable myelination in the distal nerve stumps. Poor myelin width in the Decell + SC group could be attributed to distal degeneration due to the presence of increased myelin debris (~60% more myelin debris at 12 weeks compared to 8 weeks).

Fiber distribution data showed that the Unprocessed nerve graft group and the Decell group had regenerated thicker fibers in the range of 7-8 µm, which was absent in Detergent Decell and Decell + SC groups. Increased maturity of regenerating nerve in the Decell group shows that nerve regeneration may have preceded the Detergent Decell group, and could possibly be more effective in minimizing atrophy of muscle due to earlier reinnervation.

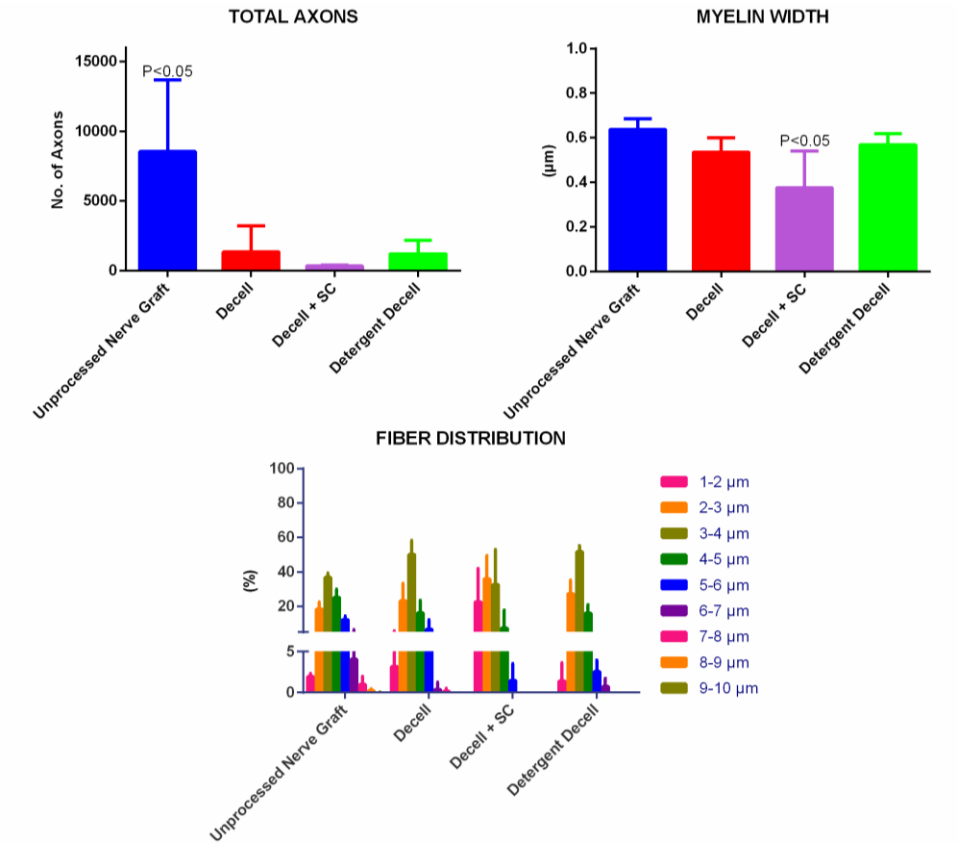

Figure 2.14 Comparison of total axons, myelin width and fiber distribution between Unprocessed nerve graft, Decell, Decell + SC and Detergent Decell groups at 12 weeks.

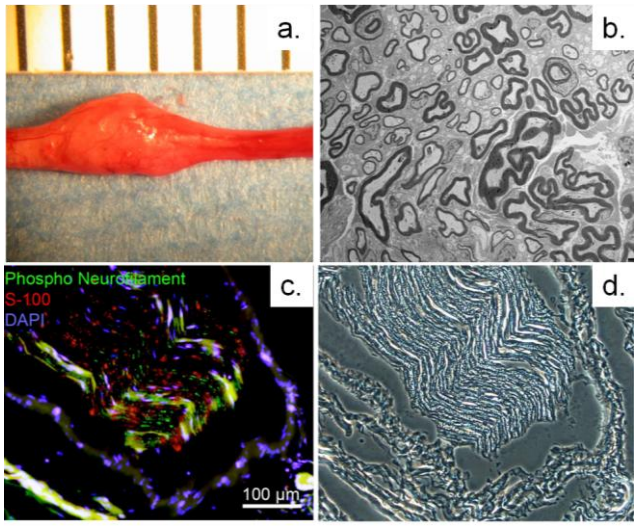

Figure 2.15 Analysis of Decell + SKPs group. (a) Swollen proximal nerve at the time of harvest. (b) TEM image of enlarged section shown in (a). (c) Proximal section stained with Phospho Neurofilament (axons), S-100 (Schwann cells) and Nuclei (DAPI). (d) Phase contrast image of stained section.

Throughout the experiments, Decell + SKPs group did not show any regeneration into the distal nerve stump. Some cases showed swelling at the time of harvest as shown in Figure 2.15a. TEM imaging of the section (Figure 2.15b) showed random orientation of fibers inside which appeared similar to a neuroma. We found that axons at the proximal stump may have been blocked from entering into grafts by multiple cell layers as seen in Figure 2.15c. Overall, supplementation of Decell grafts with SKPs was found to be deleterious to nerve regeneration.

As expected, the Silicone Tube group did not initiate nerve regeneration throughout the experimental duration, making it a "no re-growth" model.

Although studies on small animal models have been successfully translated into clinical practices (Kale et al., 2011), one should take utmost care while extrapolating data (Sunderland et al., 2004). For this study, 6 animals per group were used to obtain a power of 0.80 to detect 50% differences between the experimental groups, which has been shown to make an

observable difference when translated for clinical use (Kawamura et al., 2010). Detecting 50% difference with a 100% standard deviation can be extremely powerful, as approximately 30% of original motor neurons can impart normal muscle function (Tötösy de Zepetnek et al., 1992; Lutz et al., 2000; Witoonchart et al., 2003). However, comparison of tetanic specific tension did not yield a significant difference between the groups despite showing a trend towards difference (Figure 2.9). For detecting small effect sizes as seen in this case, increasing the sample size can result in increase in the power of an experiment by reducing type II errors.

2.4 Summary

We successfully demonstrated a detergent-free nerve decellularization method, that promotes functional nerve regeneration across a critical injury. We leveraged the ability of Schwann cells present inside a freshly harvested nerve to initiate Wallerian degeneration *in vitro*, which reduced myelin and cellular components in the Decell grafts and provided a favorable environment for the regenerating axons. Exogenous Schwann cell seeded grafts showed promise at earlier time points, but were not a preferred choice as the group showed degeneration at later time points. Our data with SKPs seeded grafts showed that these undifferentiated adult skin derived stem cells were deleterious to nerve growth. The most interesting experiment involving the established detergent processing technique (Detergent Decell grafts) revealed that although nerves regenerated into the distal nerve stumps, there was no functional recovery of target muscles. The overall results from our experiment suggest that the detergent-free decellularized nerve grafts (Decell grafts) were sufficient to promote functional regeneration across a long gap nerve injury.

Unprocessed nerve grafts were the best among all the groups in the experiment, but the limitations associated with them make room for improvement of the decellularized grafts presented in this work. Factors that govern regeneration of nerves across a long gap will be studied in chapter 3, and will be later utilized for improving regeneration across a long gap injury using detergent-free decellularized nerve grafts.

CHAPTER 3

MOLECULAR PROFILING OF REGENERATIVE VS. NON-REGENERATIVE NERVE INJURY

3.1 Introduction

Peripheral nerve injuries that require surgical intervention account for ~550,000 patients each year in the United States alone (published by Magellan Medical Technology Consultants, Inc., MN). This enormous clinical need drives peripheral nerve regeneration research (Yannas et al., 2007). The PNS has an inherent capacity to regenerate to a certain extent when subjected to injury. In rats, it has been demonstrated that inside nonporous silicone tube conduits, the PNS readily regenerates up to a distance of 10 mm between the proximal and distal nerve stumps, and no regeneration is observed if the gap is greater than or equal to 15 mm (Lundborg et al., 1982a). Numerous engineering and biological techniques have been employed to induce nerve regeneration (Siemionow et al., 2010). Due to variability in properties and influence of multiple unknown factors that mediate nerve growth, we sought to develop a growth or no-growth injury model, which either always grows or never initiates nerve regeneration. A growth vs. no-growth model of nerve injury will be ideal for determining key molecular differences between a regenerative injury and a non-regenerative nerve injury (no evidence of regeneration).

For establishing the growth vs. no-growth model, one of the major factors that was taken into consideration was to minimize the influence of the conduit on nerve regeneration. A silicone tube is biologically inert and has been widely used for nerve regeneration studies (Lundborg et al., 1982b; Williams et al., 1983). For a regenerative nerve gap, a 1.2 cm silicone tube was used to form an 8 mm nerve gap after implantation. The regenerative nerve injury will be referred to as short gap henceforth. A non-regenerative gap, which will be referred to as a long gap, was formed using a 3.5 cm silicone conduit with a 30 mm nerve gap after

implantation. A 30 mm gap was selected for creating a long gap injury since it is non-regenerative and is conserved across all species (Strauch et al., 2001). There was no initiation of nerve regeneration in this setting for up to 16 weeks as described in chapter two (Silicone Tube group), making it suitable for comparison with the regenerative short gap. Figure 3.1 shows a schematic representation of the growth vs. no-growth nerve injury model.

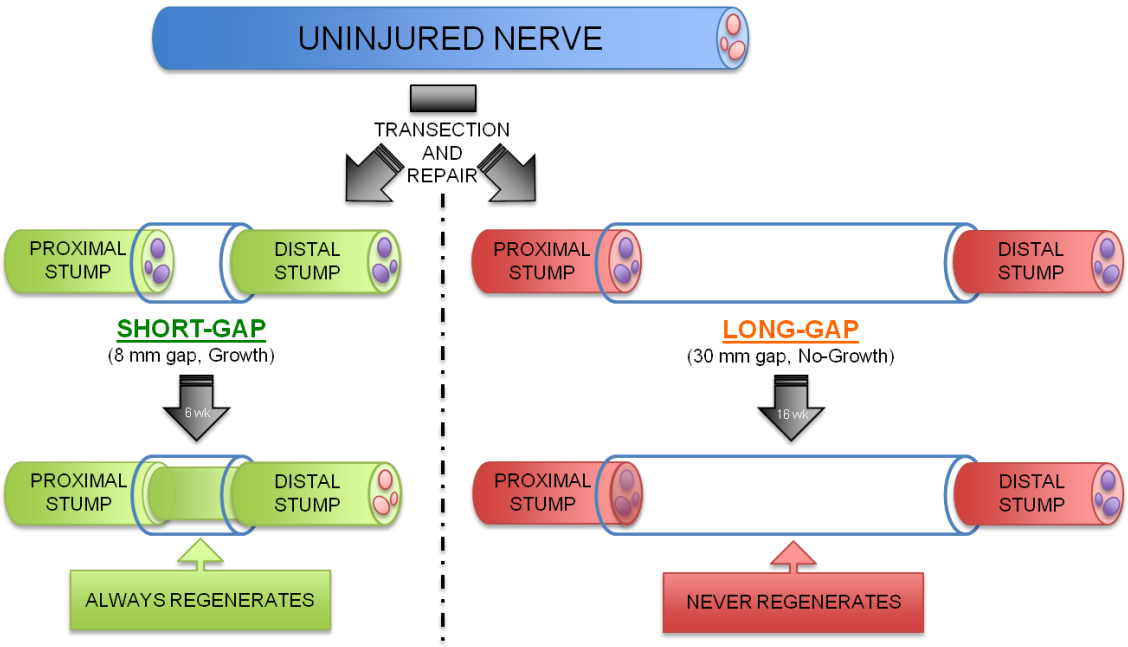

Figure 3.1 Schematic representation of the growth vs. no-growth nerve injury model using silicone tube conduits to differentiate a short gap from a long gap injury

The primary purpose of the growth vs. no-growth model described in this chapter is to differentiate a short gap injury from a long gap injury using molecular biology techniques (RT-PCR). We hypothesized that there is a difference in molecular signature between a regenerative and a non-regenerative injury. Successful demonstration of difference in gene regulation can be used to select biologic and pharmacologic compounds that can be used to improve nerve regeneration in the clinical setting.

3.2 Experimental Section

All animal procedures described in this chapter were performed as per approved Institutional Animal Care and Use Committee (IACUC) protocols at the University of Texas Southwestern Medical Center at Dallas, Texas. Rats were anesthetized using intraperitoneal (IP) injection of drug cocktail containing ketamine hydrochloride (75 mg/kg) and dexmeditomidine hydrochloride (0.5 mg/kg), and euthanized using IP injection of sodium pentobarbital (120 mg/kg). Subcutaneous injection of buprenorphine (Buprenex) was administered for pain care after survival procedures and chewable tablets of carprofen (Rimadyl) were placed in the cage for analgesia.

3.2.1 Conduit Implantation

Silicone tube conduits (1.6 mm ID) were used to create the short gap and long gap injuries in rats (male, Lewis, 250-300 g). Conduits were trimmed to desired length, rinsed in DD water and sterilized in an autoclave before implantation procedures.

Both short gap and long gap conduits were filled with 3D collagen cell culture system (Millipore, USA) using a sterile micropipette, and the collagen was allowed to gel inside a cell culture incubator at 37 °C for 45 min. At the time of implantation, the right hind limb of anesthetized rats was shaved and sterilized using 70% alcohol prep pads and betadine. Sciatic nerve was exposed and transected at mid thigh level just proximal to trifurcation. Proximal and distal nerve stumps were inserted ~2 mm into both ends of the tube to form either a short gap or a long gap injury, and held in place using 7-0 Prolene suture (Ethicon, USA).

3.2.2 Time Point Selection

To evaluate the difference in molecular profile between a long gap and a short gap injury, we harvested samples at 4 days and 7 days post-implantation.

The 7 day time point was selected based on previous electrophysiological experience (Garde and colleagues), as a regenerative electrode array implant in a short gap could record

nerve activity as early as 7 days in certain cases (Garde et al., 2009). This could be possible only when the nerve has regenerated out of the proximal stump towards the distal nerve.

3.2.3 Comparison of Short Gap vs. Long Gap Injury Using IHC

To study whether there is a difference in tissue response between the short gap and the long gap injury at 7 days, proximal stumps were harvested and immersion fixed in 4% paraformaldehyde overnight and washed in PBS. Blocks of the nerves were embedded in OCT for longitudinal sectioning in the middle of the nerves. 10 µm sections were stained with antibodies against axons (β Tubulin; Sigma Aldrich, USA), macrophages (CD68; Millipore, USA) and nuclear counterstain (DAPI; LifeTechnologies, USA).

To evaluate the number of cells near the proximal stumps of short gap and long gap injury at 4 days, the 3D collagen gel from inside the lumen of conduits was harvested and fixed in 4% paraformaldehyde and washed in PBS. Samples were embedded in OCT to obtain cross-sections. The collagen sections were stained with DAPI to quantify and compare the cell density of recruited/migrated cells.

3.2.4 Implantation for Molecular Analysis

To differentiate difference in mRNA levels between the short gap and long gap injury, animals were prepared as described previously. Short gap and long gap conduits were implanted in the right hind limb of rats (n=3 per group per time point). One set of rats was harvested at 4 days and the other was harvested at 7 days post-implantation, yielding proximal and distal nerve stumps of short gap and long gap injury at multiple time points. To prevent any degradation of mRNA, nerve stumps were collected in RNAlater solution (Qiagen, USA) for performing reverse transcription polymerase chain reaction (RT-PCR). For comparison purposes, uninjured sciatic nerves were harvested from donor rats in RNAlater solution.

3.2.5 RT-PCR of Nerve Stumps

All components used in this section were purchased from Qiagen, USA, unless otherwise noted. DNase/RNase free tubes were used for collection and processing of nerve

samples. Samples were weighed, added to a micro-centrifuge tube containing 5 mm stainless steel beads, and 650 µl of tissue lysis buffer was added. The tubes were balanced and placed in a tissue lyser to completely lyse the nerve samples. Phenol was removed from the lysis buffer by centrifuging the samples with 200 µl of chloroform. Samples free of phenol were processed using the RNeasy micro kit. Any liquid contamination during the processing was carefully eliminated by pipetting. A Picodrop spectrophotometer was used to analyze the RNA yield and purity obtained by the extraction process.

To prepare the complementary DNA (cDNA), 1 mg/ml of RNA was mixed with DNase/RNase free de-ionized (DI) water to obtain 8 µl of solution. Contents were transferred into new PCR tubes, and 2 µl gDNA elimination buffer was added to obtain 10 µl of total volume. Samples were transferred to a thermal cycler for 5 min at 42 °C to eliminate any gDNA contamination. All samples were placed at 4 °C for 3 min to eradicate gDNA eliminator effect. The tubes were subjected to thermal cycle of 42 °C for 15 min, 95 °C for 5 min and 25 °C for 1 min to synthesize cDNA. All samples were placed in a pre-cooled plate (-20 °C) and 91 µl of DI water was added to the samples.

PCR mix was made by taking 102 µl of cDNA in 1248 µl of DI water and 1350 µl of 2xSAB master mix. 25 µl of samples were added to each well and SYBR green was selected. DNA Taq polymerase was activated at 1 cycle for 10 min at 95 °C, followed by 40 cycles 15 s at 95 °C, 1 min 60 °C was performed to collect fluorescence data.

All PCR samples were normalized with uninjured nerve mRNA levels and expressed as fold regulation compared to normal.

3.2.6 Analysis of Selected Genes

To study the difference between a short gap and a long gap nerve injury, targets were selected based on type of cells, regenerative markers, neurotrophic factors that have shown to influence nerve regeneration (e.g. stem cell markers, extracellular protein markers and inflammatory cell and cytokine markers). The molecular profile of short gap and long gap injury

obtained from RT-PCR data will be used to differentiate the two injuries, and further our understanding of early events that control nerve regeneration.

3.3 Results and Discussion

3.3.1 Short Gap vs. Long Gap IHC

After 7 days of conduit implantation, we observed the presence of axons near the lesion site of a long gap injury and beyond the lesion in the short gap injury (Figure 3.2). When a peripheral nerve is subjected to injury, axons distal to the site of injury undergo Wallerian degeneration. There is recruitment of macrophages that phagocytose degenerating myelin and axonal fragments, to the injury site and the distal nerve stump (Hirata et al., 1999). We investigated the recruitment of macrophages at the proximal nerve stump using IHC techniques (Figure 3.2). It was observed that the macrophages are confined to the very distal end in the short gap injury, but an extended region of macrophages was seen in the long gap injury. This is indicative of difference in immune response between the two injuries, which can be evaluated using molecular biology techniques. We also observed that multiple layers of cells (DAPI) were formed in the surrounding tissue at the regenerating end of the nerves. Interestingly, there was an evident tissue outgrowth beyond the lesion site in the short gap injury, which was absent in the long gap injury.

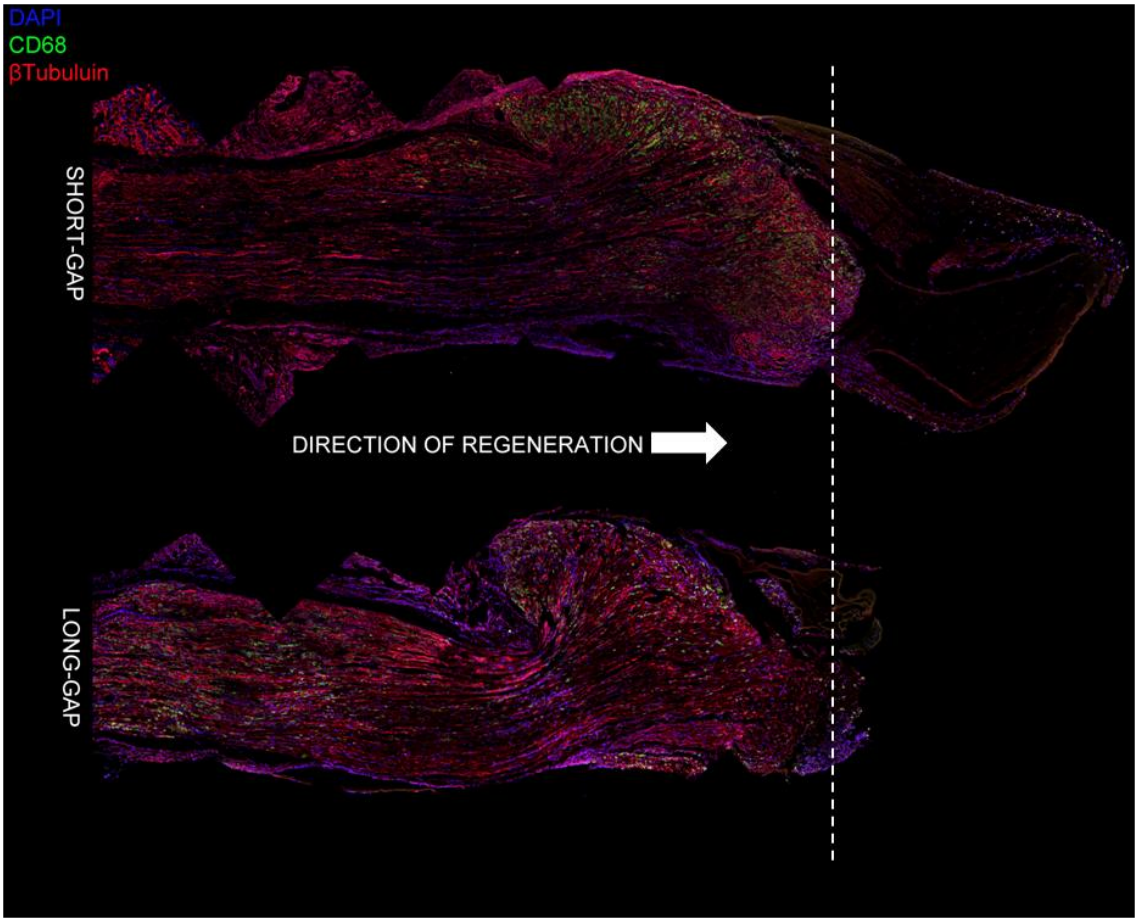

Figure 3.2 Histological evaluation of short gap and long gap proximal stumps at 7 days. Longitudinal sections were stained with β-tubuluin (axons), CD68 (macrophages) and DAPI (Nuclei). Dotted line shows the transection site.

3.3.2 Cell Recruitment/Migration Near Proximal Stumps

Nerve injury leads to Wallerian degeneration which requires recruitment of immune cells for clearing cell fragments and myelin. This process also creates a favorable environment that promotes growth of axons from the regenerating proximal stump. We observed that a short gap recruited higher density of cells than a long gap injury as early as 4 days after injury (Figure 3.3). These cells were observed distal to the lesion site inside the lumen of the conduit. This was investigated because a regenerative response could be linked to the type of cells recruited at early stages of regeneration.

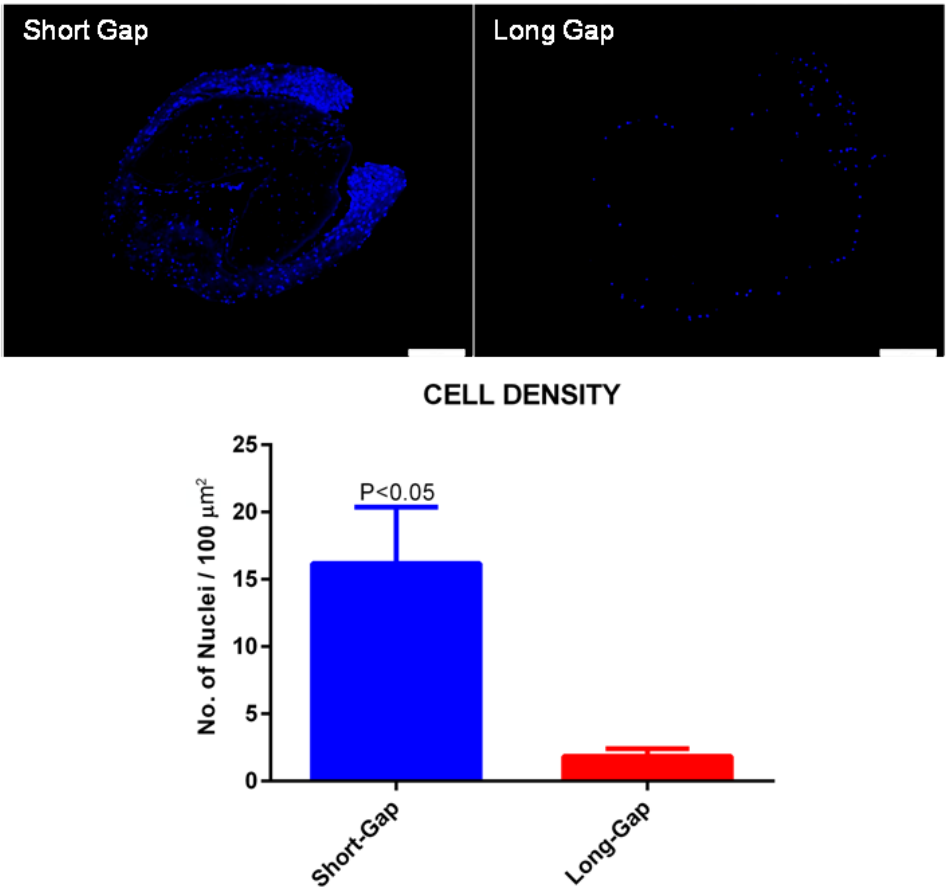

Figure 3.3 DAPI stained images of short gap and long gap injury inside the conduit near the proximal stump. Graph comparing cell density between the two injuries. Data shown as Mean ± SD, compared using Student's t-test

3.3.3 PCR Data Analysis

In peripheral nerves S100β is exclusively found in the Schwann cells (Spreca et al., 1989), which provide growth factors and extracellular matrix proteins (ECM) to promote nerve regeneration after injury (Shen et al., 2001). We evaluated the expression level of this specific marker to differentiate the short gap and the long gap nerve injury (Figure 3.4). We observed that Schwann cells tend to react more rapidly to injury in a short gap than in the long gap by reducing the expression levels further at 4 days. Denervated Schwann cells undergo dedifferentiation and down-regulate S-100, which is restored after reinnervation of Schwann

cells (Magill et al., 2007). We found that the Schwann cells in the short gap readily dedifferentiate into a more immature state to support regenerating axons, which seems to be slower in the case of a long gap injury.

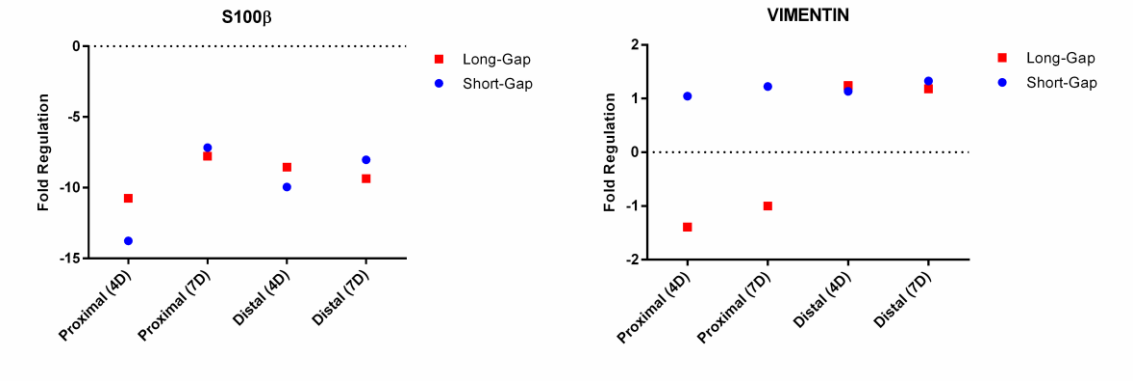

Figure 3.4 PCR data for comparison of resident cells between a short gap and long gap at 4 days and 7 days post-implantation

Endoneurial fibroblasts form a major population of cells in the peripheral nerves, that are vimentin positive. These cells have been shown to produce nerve supporting growth factors upon stimulation by macrophage secreted factors (Spreyer et al., 1990). Research shows that fibroblasts in the peripheral nerves are derived from neural crest stem cells during development (Joseph et al., 2004) and aid in formation of the nerve tissue. Our data shows that the expression of vimentin is up-regulated in the short gap compared with the long gap as seen in Figure 3.4, possibly indicating new nerve tissue formation after injury. Altering fibroblast response in a long gap might induce a more regenerative microenvironment for developing new nerve tissue.

Regenerating axons navigate to the distal targets using a specialized structure, the growth cone, which forms the distal tip. Synthesis of growth associated protein-43 (GAP-43) at the growth cone is elevated during regeneration (Skene et al., 1986; Reynolds et al., 1991). The expression level of GAP-43 does not vary drastically between the two groups, but there is a

steady up-regulation from 4 days to 7 days in the short gap injury, suggesting a regenerative profile (Figure 3.5).

Upon injury, the Schwann cells lose contact with axons, dedifferentiate and acquire a non-myelinating phenotype. During this process, the myelin basic protein (MBP) mRNA levels have shown to be down-regulated (Stoll and Müller, 1999), which is similar to what we found in Figure 3.5. The response to injury in both cases seem to be similar in terms of MBP down-regulation, suggesting that the Schwann cell dedifferentiation at 4 days follows a similar pattern.

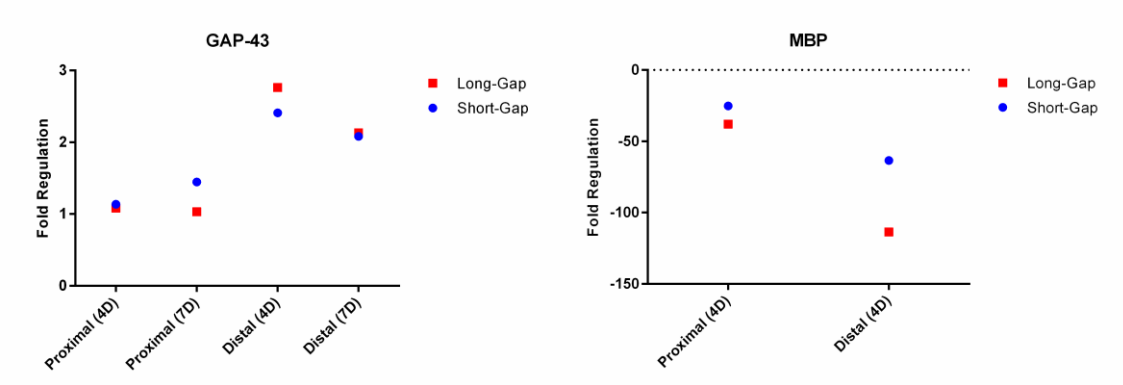

Figure 3.5 PCR data showing growth associated markers (GAP-43), and myelin associated markers (MBP)

Nestin, a neural stem/progenitor cell marker (Drapeau et al., 2005), seems to stay below baseline in both cases showing that these cells may not be playing an active role at early time point of regeneration (Figure 3.6).

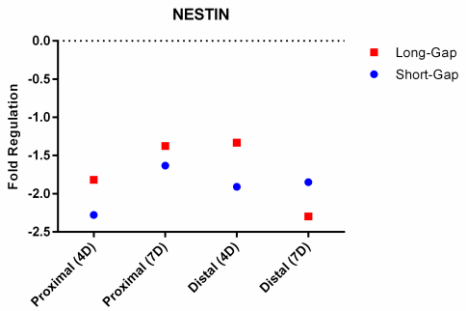

Figure 3.6 Expression of neural progenitor marker (Nestin) at 4 days and 7 days post-implantation

When peripheral nerves are subjected to injury, receptors for brain derived neurotrophic factor (BDNF) are up-regulated, and play a vital role in axonal growth (Zhang et al., 2000). BDNF has been used to aid in nerve regeneration (Frostick et al., 1998; Terenghi, 1999; Wilhelm et al., 2012). Our data suggests that BDNF does not vary between the regenerative and the non-regenerative condition at 4 days, possibly indicating no controlling effect on initiation of nerve regeneration (Figure 3.7).

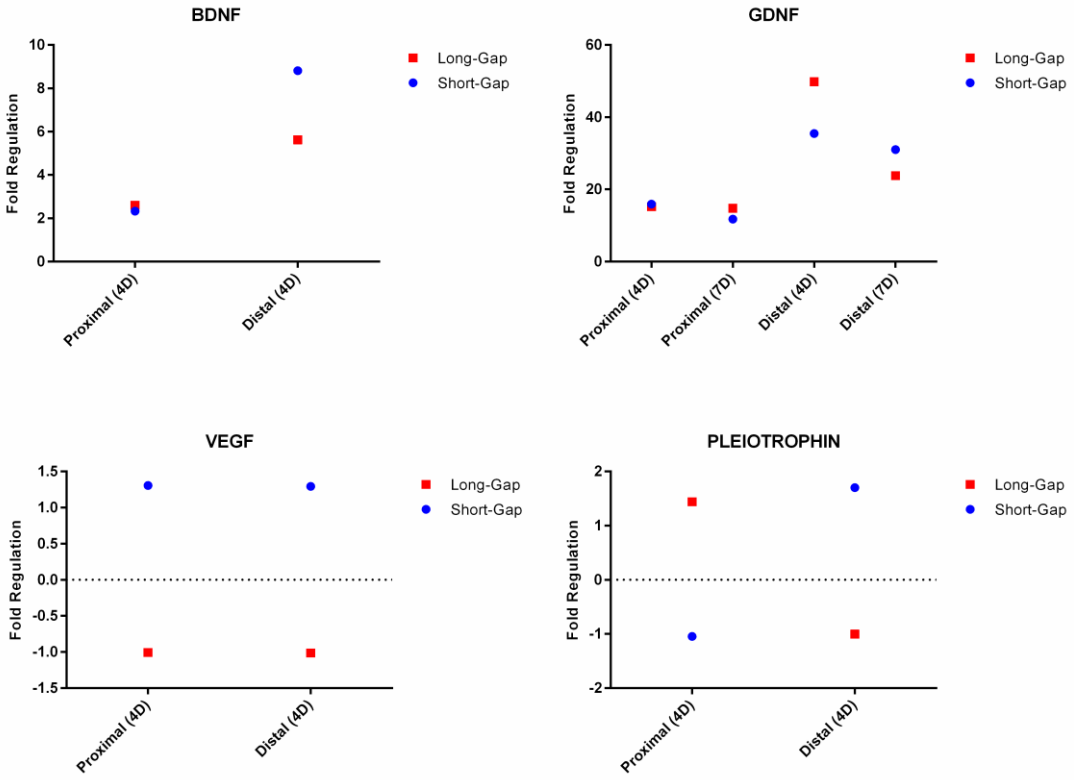

Figure 3.7 Growth factors that have been shown to aid in nerve regeneration. Expression difference between a short gap and a long gap injury from PCR data

Glial cell line-derived neurotrophic factor (GDNF) has been used to promote nerve regeneration (Fine et al., 2002), and has been shown to be a potent survival factor for motor neurons (Henderson et al., 1994). Our data in Figure 3.7 shows that the expression level of

GDNF is similar in both groups, suggesting that GDNF might not be a key element at early stages of regeneration.

Angiogenesis has been shown to play a vital role in nerve regeneration using a highly specific mitogen for endothelial cells, vascular endothelial growth factor (VEGF) (Hobson et al., 2000). Other than effects on angiogenesis, VEGF stimulates growth of axons, and enhances proliferation and survival of Schwann cells (Sondell et al., 1999). We investigated the expression level of VEGF mRNA in the growth vs. no-growth nerve injury model and found that a regenerative injury shows up-regulation of VEGF vs. seeing an opposite effect in the non-regenerative environment (Figure 3.7). A possible role for VEGF in formation of neo-vasculature is observed in the regenerative gap to provide support to the regenerating tissue.

Pleiotrophin (PTN) belongs to the heparin-binding growth factor family, and it is expressed around developing axons (Blondet et al., 2005). PTN has been used to enhance regeneration of myelinated axons, and it is up-regulated in acutely denervated nerve stumps (Mi et al., 2007). However, we found that the PTN mRNA levels are different between the two groups, but PTN is down-regulated in the short gap condition as compared with the long gap, where it is up-regulated (Figure 3.7). It is an interesting finding that a growth promoting factor is down-regulated in the regenerative injury and up-regulated in the non-regenerative long gap injury.

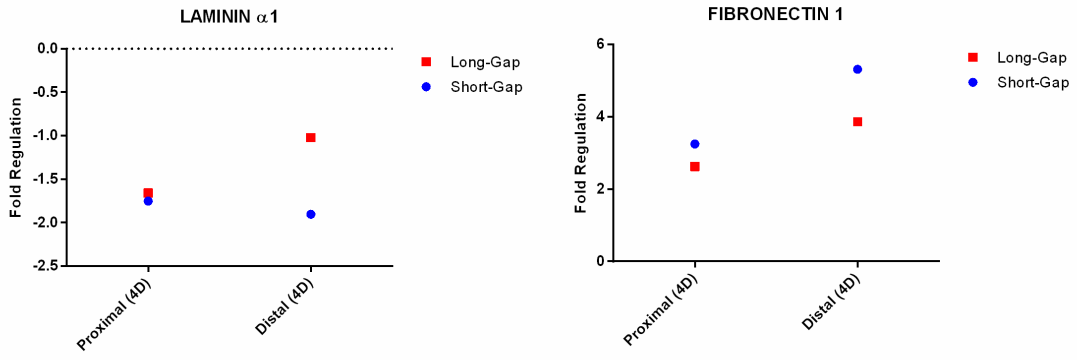

Figure 3.8 PCR data showing difference in expression of ECM proteins

Research suggests that using ECM proteins can alter the response to nerve injury and enable faster regeneration (Bellamkonda, 2006). Neurites interact with ECM proteins through integrins, that leads to signal transduction, growth regulation, differentiation and other vital biological processes (Damsky and Werb, 1992). Two ECM proteins, laminin and fibronectin, that have been shown to promote nerve regeneration (Wang et al., 1992; Tong et al., 1994) were studied using our model (Figure 3.8). The mRNA levels were similar in both short gap and long gap cases. This may have been observed since the ECM proteins are presented at later stages of regeneration, and not at early regenerative stages.

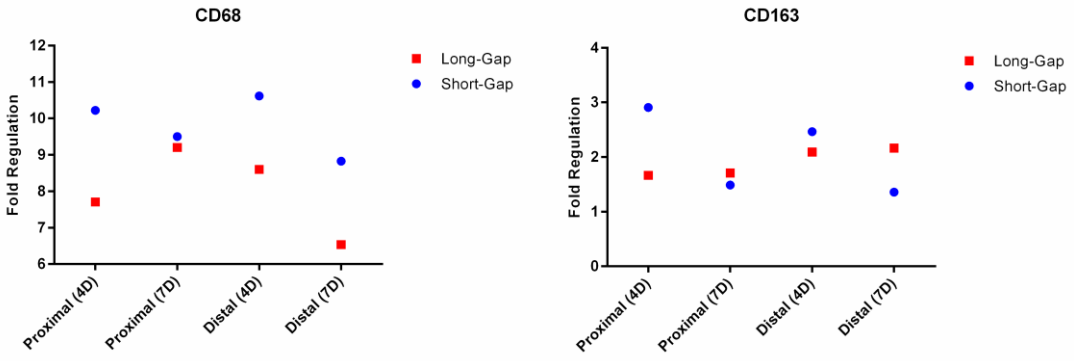

Figure 3.9 Data showing difference in immune cell response to short gap and long gap injuries

In the prior section, Figure 3.2 showed that a regenerative nerve injury recruits macrophages specifically to the lesion site, which is not the case with a non-regenerative environment. The mRNA levels for CD68 in Figure 3.9 supports the data obtained previously. The short gap environment, which regenerates, has the ability to recruit exogenous immune cells to clear fragments and produce growth factors at 4 days. The levels, however, are similar to a long gap environment at later stages, indicating a delayed response.

M2 macrophages (CD163) support tissue repair, and produce anti-inflammatory cytokines while reducing destructive microenvironment (Mokarram et al., 2012; Ydens et al.,

2012). From Figure 3.9, we can infer that wound healing response in a regenerative injury initiates at early time points, and a non-regenerative injury has a stable response level in the initial stages after injury.

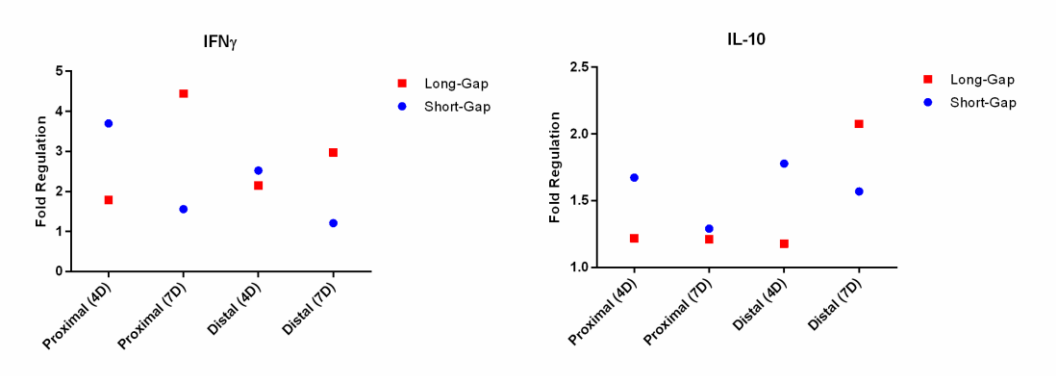

Figure 3.10 Differential expression of cytokines obtained from PCR data.

Interferon Gamma (IFNγ) is a potent major histocompatibility complex inducing factor, and elicits response to axonal damage (Olsson et al., 1989). IFNγ expression is elevated during Wallerian degeneration, and activates a pro-inflammatory phenotype in recruited macrophages and other immune cells (Stoll et al., 2002). IL-10 expression is observed during Wallerian degeneration, and it may stimulate infiltrating macrophages to produce inflammatory cytokines (Taskinen et al., 2000). Figure 3.10 shows that the expression of IFNγ is varying inversely between a short gap and a long gap injury at 4 days and 7 days post-lesion. It could be indicating that the regenerative state of a nerve is enhacned if there is a burst of inflammation at earlier stages than later stages of injury. IL-10 expression in the short gap is elevated two-fold above the long gap.

3.4 Summary

We successfully developed and characterized a growth vs. no-growth nerve injury model to study nerve regeneration in a well established animal model. The contrast between the always regenerative state of a short gap injury can be compared with the always non-regenerative long gap injury in terms of cellular and molecular differences to understand nerve regeneration. We demonstrated that the signals leading to cell recruitment and proliferation differ between the two injuries. The use of RT-PCR to compare regenerative vs. non-regenerative nerve injuries gave us an opportunity to obtain the molecular profile of successful nerve regeneration. Finally, we found that there is a difference in molecular signature between a regenerative short gap injury and a non-regenerative long gap injury, that may facilitate control of nerve regeneration.

CHAPTER 4

DEVELOPING IMPROVED DECELLULARIZED NERVE GRAFTS

4.1 Introduction

Peripheral nerve injuries are very common forms of traumatic injuries, that can be reconstructed by end-to-end direct repair if there is no loss of tissue. Nerve grafting is essential when tension-free end-to-end repair is not possible due to segmental tissue loss (Karabekmez et al., 2009; Guo et al., 2013). In the clinical settings, reconstruction of nerve gaps is performed using autografts. Donor site morbidity, formation of painful neuroma, loss of function at the harvest site and tissue scarring are some of the major limitations associated with the use of autografts (Katayama et al., 2006). To address the limitations of traditional treatment procedures, alternative strategies such as the use of decellularized nerve grafts have been used clinically (Cho et al., 2012; Guo et al., 2013). However, the use of decellularized nerve grafts have been limited to repair of short nerve defects (Berrocal et al., 2013).

A detergent-free decellularization method for processing nerve grafts was developed and evaluated for repairing long nerve gap defects (35 mm). We demonstrated that the detergent-free decellularized nerve was able to support axonal growth over the entire length and form functional connections with target muscles. The novelty of the processing technique is the initiation of Wallerian degeneration *in vitro*, which possibly reduces inhibitory components and promotes nerve regeneration. Wallerian degeneration forms a growth supportive environment after nerve injury, and the number of regenerating axons dictates the degree of functional recovery (Hontanilla et al., 2006). We found that only ~30% of axons regenerated to the distal nerve stumps using the Decell grafts, which is consistent with clinically used decellularized nerve grafts tested in rat models (Whitlock et al., 2009).

The aim of this work was to develop improved detergent-free decellularized nerve grafts, that can promote better axonal regeneration across a 35 mm long nerve gap injury as compared with the previously described Decell and Detergent Decell grafts. We hypothesized that by recapitulating a short gap environment in the long gap condition, initiation of nerve regeneration can be obtained (Figure 4.1). We carefully selected specific compounds from the RT-PCR analysis of a growth vs. no-growth nerve injury model and found that these compounds were effective in eliciting regeneration across a long gap. Since the aim was to develop improved decellularized nerve grafts, we optimized processing time to eliminate cellular components and removed inhibitory CSPGs to facilitate nerve regeneration. We also tested the improved decellularized nerve grafts supplemented with selected compounds that induced nerve regeneration across a long gap. The improved grafts were found to be better than the previous Decell grafts and one of the compound supplemented grafts showed robust regeneration and was comparable to unprocessed nerve graft.

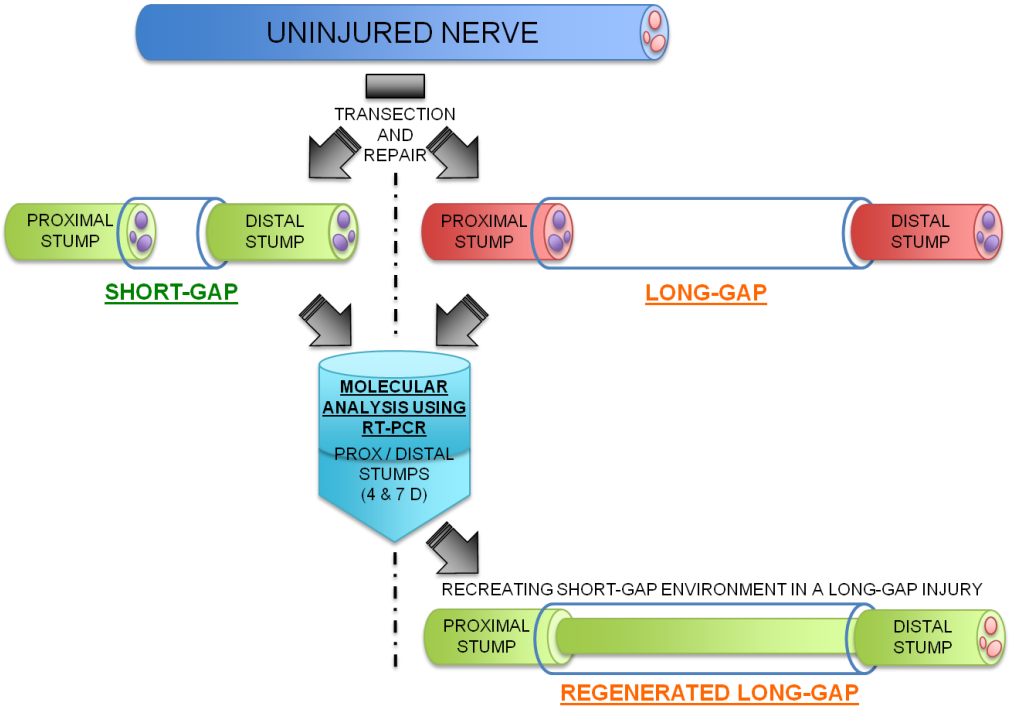

Figure 4.1 Schematic representation of the hypothesis

4.2 Experimental Section

All animal procedures were performed as per approved Institutional Animal Care and Use Committee (IACUC) protocols at the University of Texas Southwestern Medical Center at Dallas, Texas. Rats were anesthetized using intraperitoneal (IP) injection of drug cocktail containing ketamine hydrochloride (75 mg/kg) and dexmeditomidine hydrochloride (0.5 mg/kg), and euthanized using IP injection of sodium pentobarbital (120 mg/kg). Subcutaneous injection of buprenorphine (Buprenex) and chewable tablets of carprofen (Rimadyl) were placed in the cage for post-operative analgesia.

4.2.1 Selection of Potential Pro-Regenerative Compounds

From the PCR analysis of our growth vs. no-growth nerve injury model, we selected three compounds to test regeneration across a critical nerve injury. All compounds were purchased from Tocris Biosciences, UK. Compound A, Compound B and Compound C were chosen.

4.2.2 Enhancing Regenerative Nerve Injury

To study whether a regenerative injury can be improved by supplementing the conduits with selected compounds, we used a 8 mm gap defect (12 mm tube length, n=3 per group) and individually tested all three selected compounds. We mixed the compounds with 3D collagen gel that is used as a carrier and evaluated regeneration at 6 weeks. To evaluate nerve regeneration, quantitative histomorphometry was performed on distal nerve stumps as described in section 2.2.11.

4.2.3 Nerve Regeneration Across Critical Gap

We used a 20 mm gap (25 mm conduit length, n=6 per group) length to test the ability of selected compounds to elicit nerve regeneration across a critical gap. Compounds were mixed with 3D collagen used to fill the lumen of conduits. Conduits were implanted across the right sciatic nerve transected at mid-thigh level. Animals were harvested at 16 weeks after

implantation to analyze nerve regeneration in the distal nerve stumps using quantitative histomorphometry.

4.2.4 Improved Decellularized Nerve Grafts

To optimize detergent-free decellularized nerve grafts that can improve nerve regeneration, we tested multiple culture medium and degeneration techniques that induced efficient myelin degradation. Other factors taken into consideration include mechanical integrity for implantation and internal architecture for supporting axonal growth. This protocol describes the most effective condition, that we used for processing nerve grafts.

Sciatic nerves were harvested from donor rats as described in section 2.2.1, and sutured onto rubber holders to retain length during processing. For in vitro Wallerian degeneration, nerves along with rubber holders were transferred into 15 ml conical tubes containing 7 ml DMEM10, and cultured for 3 weeks (37 °C and 5% CO_2) under constant agitation. During this time, 3 ml medium was replaced with 3.5 ml fresh medium every 3 days to replenish nutrients. Decellularization was achieved by replacing DMEM10 with PBS and agitating for 1 week in a cell culture incubator. To remove inhibitory CSPG from the decellularized nerve grafts, grafts were immersed in PBS containing ChABC (2 units/ml) for 16 hr 37 °C inside a cell culture incubator as described elsewhere (Neubauer et al., 2007). Finally, the nerve grafts were washed in PBS 3 times for 15 min each to eliminate any residual ChABC, and stored at 4 °C until engraftment.

The decellularized nerve grafts obtained by the modified detergent-free processing technique will be referred to as iDecell (improved Decell) grafts.

4.2.5 Ultra-Structural Evaluation of iDecell Grafts

TEM was used to study myelin architecture in the iDecell grafts. To study the importance of DMEM10 processing, we prepared control grafts that were agitated in PBS for 4 weeks in a cell culture incubator.

Samples of processed nerves were immersion fixed in 3% glutaraldehyde and post-fixed in osmium tetroxide, followed by embedding in Araldite 502. Ultra-thin sections were cut and stained with uranyl acetate-lead citrate solution. High magnification images were obtained to study components of nerves.

4.2.6 IHC Analysis of iDecell Grafts

Endoneurial tubes after processing were observed by fixing samples in 4% paraformaldehyde followed by embedding and cryosectioning. Cross-sections were blocked with 4% goat serum and stained with mouse anti-laminin B2 gamma 1 (D18) primary antibody, and goat anti-mouse Alexa Fluor 488 secondary antibody. Images were taken for qualitative analysis.

4.2.7 Evaluation of Myelin Clearance in iDecell Grafts

After DMEM10 processing for 3 weeks to induce *in vitro* Wallerian degeneration, samples of nerve grafts at day 0 in PBS, 3.5 days in PBS and the last day (day 7) in PBS were fixed in 4% paraformaldehyde. Cross-sections were cut in a cryostat and stained with FluoroMyelin (Invitrogen, USA) stain. For comparing the rate of myelin degradation, uninjured sciatic nerve cross-sections were used as a control.

4.2.8 Rate of Decellularization in iDecell Grafts

The 1 week PBS processing step is used to cut-off nutrient supply and induce apoptosis in the cells that were effectors of *in vitro* Wallerian degeneration. To study the effectiveness of this process, we stained nerve samples obtained in section 4.2.7 with DAPI to determine cell density. Uninjured nerve sections served as control.

4.2.9 TUNEL Assay for Detecting Apoptosis in iDecell Grafts

To study the state of cells that are remaining after completing the detergent-free decellularization process, DeadEnd™ Fluorometric TUNEL System (Promega, USA) was performed to look at apoptotic cells.

4.2.10 Experimental Setup

Regenerative potential of iDecell grafts was evaluated with and without supplemented compounds selected from PCR data. Sixteen rats (male, Lewis, 250-300 g) were randomly assigned to four groups: (1) iDecell (n=4), (2) iDecell + Comp A (iDecell grafts with Compound A, n=4), (3) iDecell + Comp B (iDecell grafts with Compound B, n=4) and (4) iDecell + Comp C (iDecell grafts with Compound C, n=4). To test whether the selected compounds were applicable to a critical nerve defect of 35 mm, iDecell grafts for Groups 2, 3 and 4 were immersed for 3 days in PBS containing respective compounds before implantation. At the time of implantation, Grafts were trimmed to 35 mm length and inserted into 3 silicone collars (7 mm length, ~2.5 mm ID) placed at proximal, mid and distal regions of the grafts and loaded with 3D collagen gel containing respective compounds. The collar was removed after the collagen solidified, leaving the collagen containing compounds secured to the graft surface. The iDecell grafts received collagen only.

4.2.11 Implantation and Harvest

All animal surgeries were performed as described previously by the same surgeon to obtain consistent results. Briefly, right hind limb of male Lewis rats were shaved and sterilized using alcohol pads and betadine. Sciatic nerve was exposed by mid-thigh muscle splitting approach and transected before trifurcation. Long-nerve grafts were looped around the anterior head of biceps femoris muscle as described earlier and secured in place using fibrin glue (Baxter, USA). Wounds were closed and regeneration across the new grafts were evaluated at 12 weeks post-implantation.

4.2.12 Evaluation of Nerve Regeneration

Muscle function tests were performed at 12 weeks post-implantation as described in chapter 2. Tetanic specific tension and wet muscle mass was used to evaluate reinnervation of gastrocnemius muscle.

To study axonal growth in the distal nerve stumps, quantitative histomorphometry was performed as described previously. Axon count, myelin width and fiber distribution were used as the parameters for comparison of nerve regeneration.

4.2.13 Statistical Data Analysis

Results were analyzed using Student's t-test between two groups with $P< 0.05$. Multiple groups were compared using one-way analysis of variance (ANOVA) with $P< 0.05$ and Newman-Keuls Post-hoc method was used for pairwise comparison (Statistica 4.5). Data is presented in terms of mean ± standard deviation (SD) if not specified.

4.3 Results and Discussion

4.3.1 Enhancing Regenerative Nerve Injury

To study whether the compounds selected from PCR data can be used to make a regenerative short gap injury better, we implanted silicone conduits with collagen containing Compound A (Comp A), Compound B (Comp B) and Compound C (Comp C). We found that Comp A group regenerated significantly higher number of axons in the short gap than the control group (silicone tube only). Although there were larger number of axons in the Comp B and Comp C groups, there was no significant difference as compared with control group (Figure 4.2). This experiment shows that there is still room for improvement in a regenerative condition, which can prove to be useful in clinical settings.

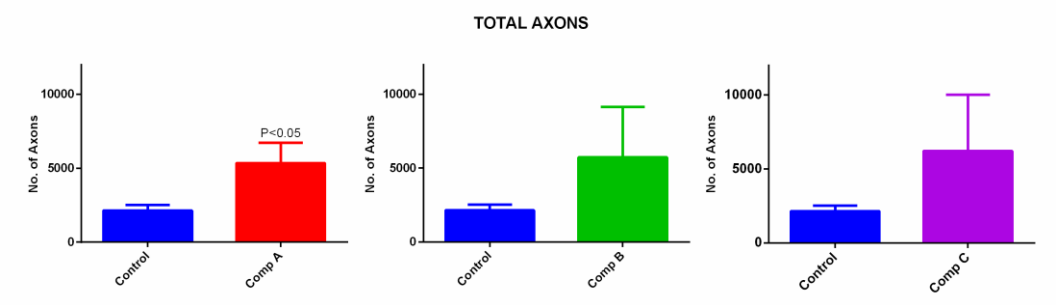

Figure 4.2 Improving short gap nerve injury using luminal delivery of selected compounds.

4.3.2 Initiating Regeneration Across a Long Gap

Regeneration across a 20 mm gap was achieved by individually testing all three compounds in the lumen of a silicone tube conduit. Axon counts of regenerated distal nerves is seen in Figure 4.3.

Historical controls show that the regeneration of myelinated axons in a 20 mm gap loaded with collagen filler extends only 4 mm beyond the proximal end (Madison et al., 1988). By using compounds selected from the PCR analysis, we were able to elicit regeneration into the distal nerve stumps. This model proved useful to test the role of selected compounds in inducing nerve regeneration across a critical defect. The enhancement of regeneration can be further tested in longer injury models that are discussed later in this work.

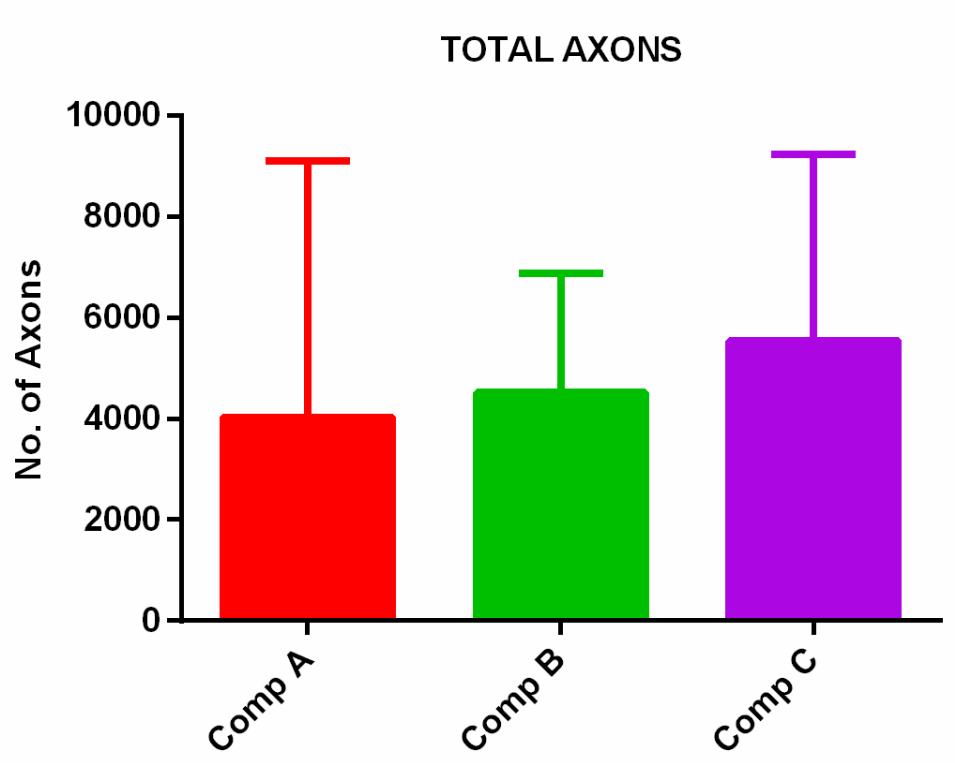

Figure 4.3 Regeneration across a 20 mm nerve gap using Comp A, Comp B and Comp C

4.3.3 TEM Analysis of iDecell Grafts

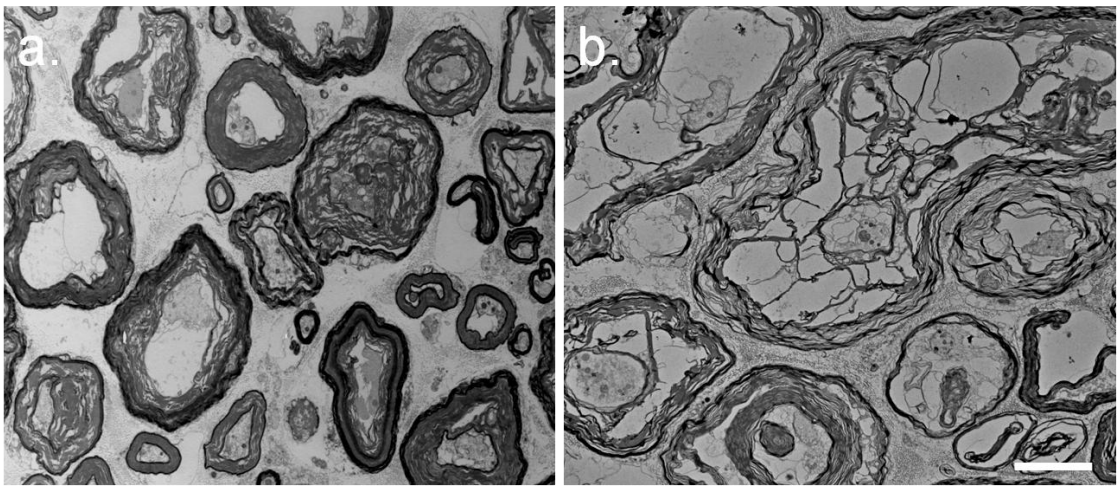

Figure 4.4 TEM images of (a) PBS treated grafts and (b) iDecell grafts. Scale bar 5 µm.

Effect of *in vitro* Wallerian degeneration on myelin and cellular components was analyzed using TEM. Myelin sheath in PBS only treated group (control) remained fairly intact and presence of cellular components can be seen (Figure 4.4a). iDecell grafts show improved myelin breakdown and lack of axonal components and nuclei, suggesting that the optimized detergent-free decellularization technique was effective (Figure 4.4b).

Survival of Schwann cells in the grafts during 3 week *in vitro* Wallerian degeneration plays an important role in cell-mediated myelin degradation, that is essential to obtain a regenerative environment in the iDecell grafts. The new process seems to provide better effect on myelin clearance as compared with initial processing, while retaining the mechanical properties required during implantation and regeneration.

4.3.4 Internal Structure of iDecell Grafts

Laminin staining of iDecell grafts shows defined endoneurial tubes as seen in Figure 4.5. In comparison, Schwann cell basal lamina tubes are only partially intact in *detergent processed* nerve grafts, but an ideal nerve graft should have intact endoneurial tubes to support nerve regeneration (Whitlock et al., 2009). Detergent-free decellularization technique presented

here shows advantages over detergent processed grafts in maintaining internal nerve architecture.

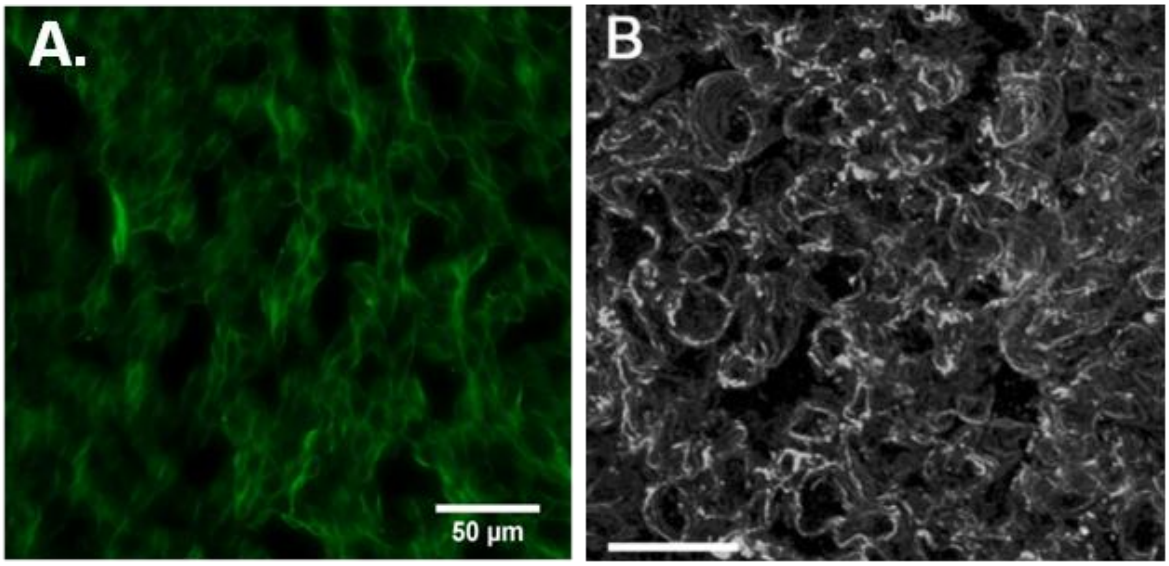

Figure 4.5 (A) Laminin staining of iDecell graft cross-sections showing endoneurial tubes. (B) Laminin staining of detergent processed grafts. Scale bar 20 µm (Whitlock et al., 2009).

4.3.5 Myelin Clearance and Decellularization

The detergent-free decellularization process showed substantial reduction of myelin after *in vitro* Wallerian degeneration (Figure 4.6). It was found that the fluorescence intensity of myelin staining was absent after 3.5 days in PBS. These results suggest that Schwann cells inside the nerve grafts were able to degrade myelin substantially after 3 weeks in DMEM10. The decellularization graph shown in Figure 4.6 suggests that by agitating and replenishing medium, cell survival inside nerve grafts is achieved.

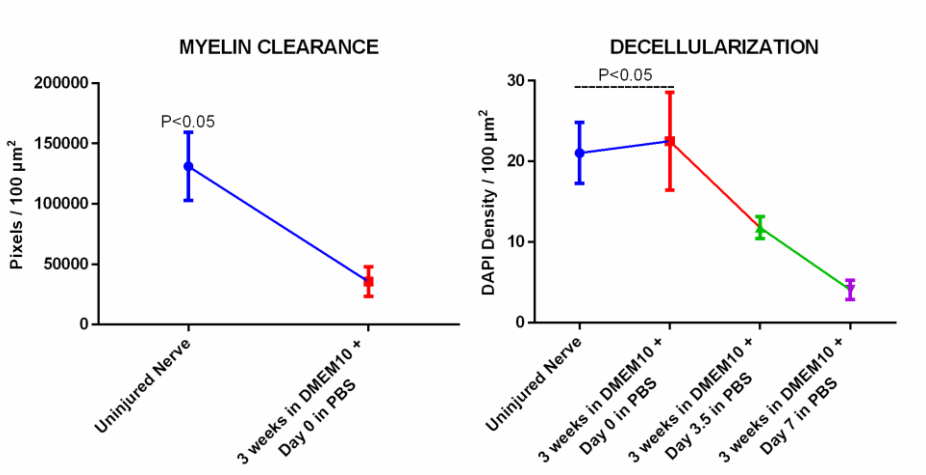

Figure 4.6 Characterization of myelin clearance and decellularization in iDecell grafts

Results of decellularization process demonstrates that by abruptly eliminating nutrient supply, a rapid reduction of cell density can be obtained (Figure 4.6). Even though there is a significant reduction of cells in the iDecell grafts at the end of processing, presence of cellular nuclei was observed. Longer PBS processing might be used to completely eliminate cellular contents from the nerve grafts.

4.3.6 Apoptotic Cells in iDecell Grafts

We found that there are some DAPI positive cells after 3 weeks in DMEM10 and 1 week in PBS. To test whether these cells are apoptotic, TUNEL staining was performed (Figure 4.7). We found that majority of nuclei in the grafts were TUNEL positive and can be eliminated upon implantation or by further PBS processing.

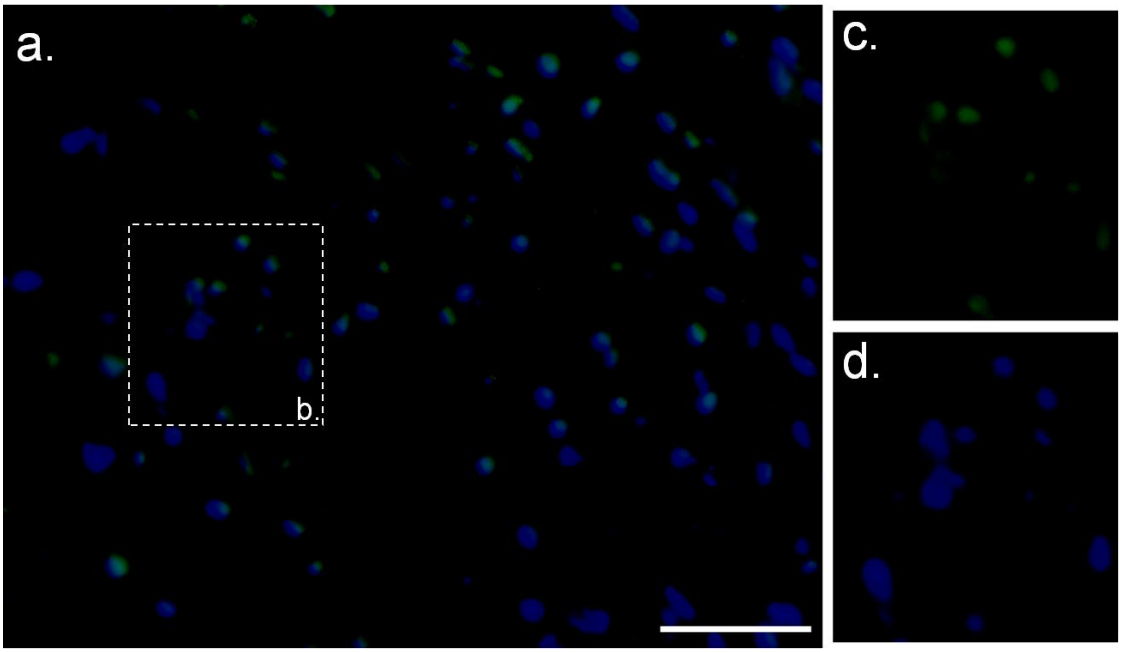

Figure 4.7 TUNEL staining of iDecell grafts after processing is completed. DAPI (blue) and TUNEL (green). (a) iDecell nerve grafts. (c) TUNEL positive signal from region selected by (b). (d) DAPI showing nuclei in region (b). Scale bar 50 µm.

4.3.7 Analysis of Functional Muscle Reinnervation

The aim of this project was to improve regeneration across a long gap using detergent-free decellularized nerve grafts. Optimization of previously used processing technique yielded iDecell grafts, that were used with or without compounds to enhance nerve regeneration.

All the groups tested had recovery of muscle function. iDecell had function in 50% cases, similar to original Decell group at 12 weeks post-implantation. iDecell + Comp C group had function in 75% of cases and some animals showed stronger tetanic tension as compared with iDecell group. There was no significant difference between iDecell and iDecell + Comp C groups in terms of tetanic specific tension and wet muscle mass (Figure 4.8). It is important to note that by delivering COMP C along with iDecell grafts (iDecell + COMP C grafts), we could increase the number of animals with functional muscle recovery.

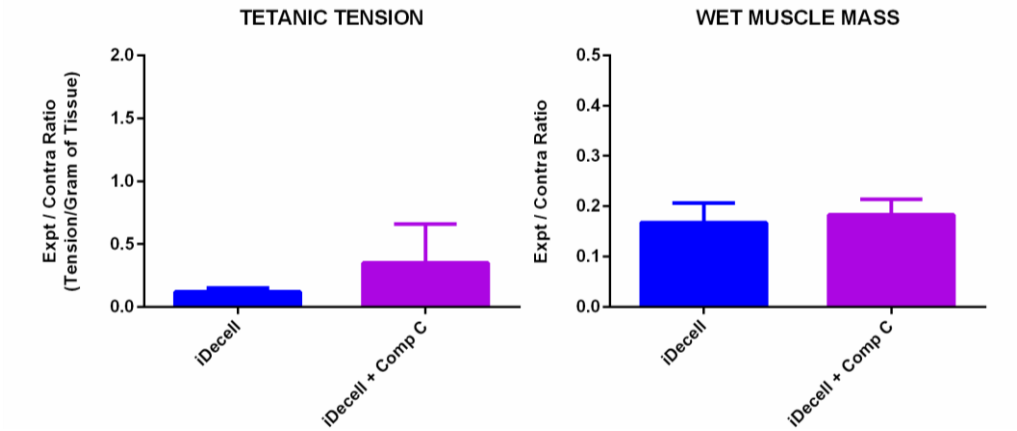

Figure 4.8 Tetanic specific tension and wet muscle mass comparison between iDecell and iDecell + Comp C group.

4.3.8 Quantification of Nerve Regeneration

All the iDecell grafts (with and without supplemented compounds) showed regeneration (100% regeneration), which by itself is a huge improvement from the previous work. Bright-field images of distal nerve stumps show that the axon regeneration in the iDecell + Comp C group was higher as compared with other groups (Figure 4.9). Thicker fibers were also observed along with thinner myelinated fibers in the iDecell + Comp C group.

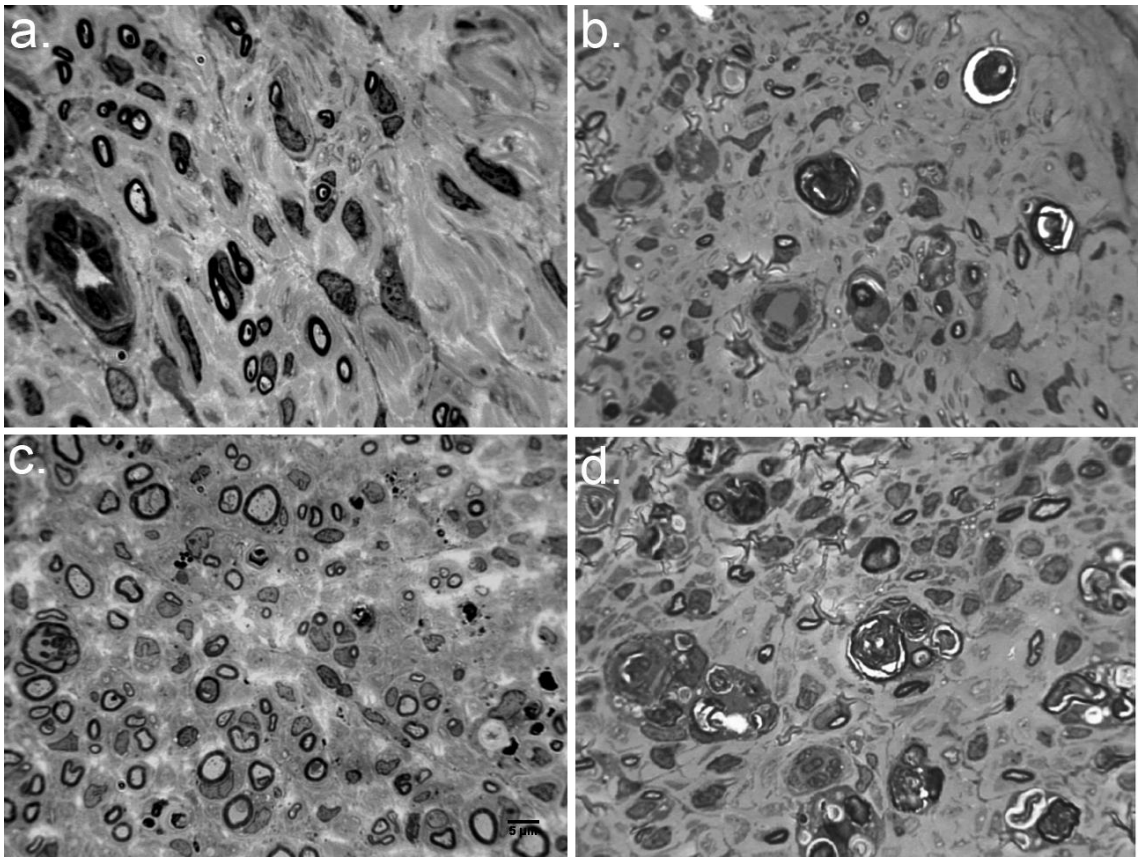

Figure 4.9 Bright field images showing regeneration in the distal nerve stumps of (a) iDecell + Comp A, (b) iDecell + Comp B,(c) iDecell + Comp C and (d) iDecell. Scale bar 5 µm.

We compared total axons, myelin width and fiber distribution among all treatments (Figure 4.10). iDecell + Comp C group showed significantly higher number of axons in the distal nerve stump. There was no significant difference in myelin width between groups, which indicates maturity of myelination was comparable among all regenerated groups. Fiber distribution data shows presence of >8 µm fibers only in the iDecell + Comp C group, possibly due to faster nerve regeneration and maturation.

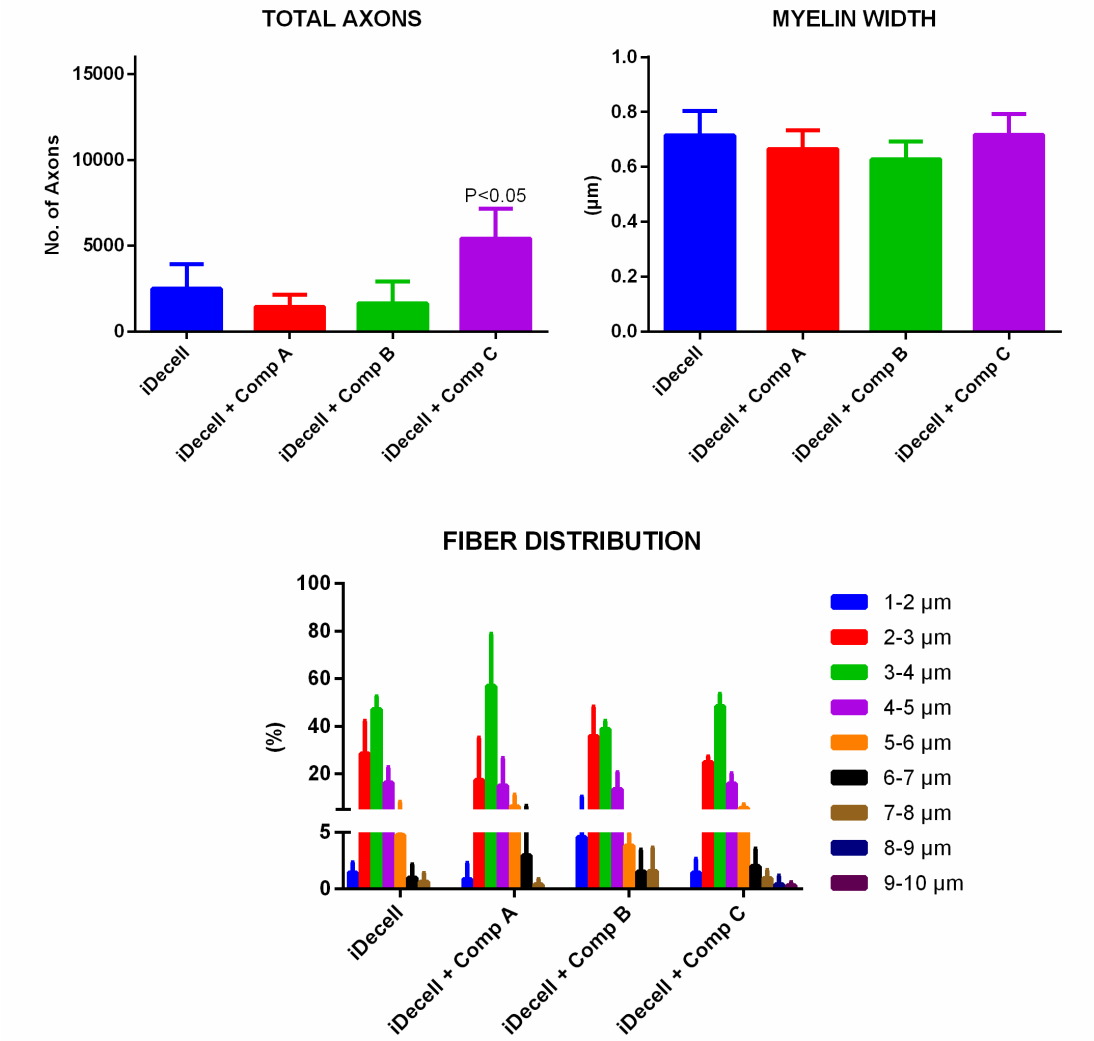

Figure 4.10 Histomorphometry comparison between groups showing total axons, myelin width and fiber distribution in the distal nerve stump.

We compared the iDecell and iDecell + Comp C groups with Decell group to see if the optimized processing technique improved nerve regeneration. The iDecell had about twice as many axons as compared with the Decell control group. iDecell + Comp C grafts had significantly higher number of axons in the distal stump (Figure 4.11).

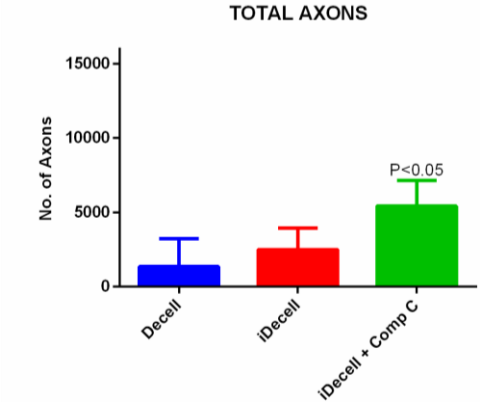

Figure 4.11 Axonal count comparison between Decell Control, iDecell and iDecell + Comp C

Finally, iDecell + Comp C group was compared with the positive control (Unprocessed nerve graft) from Chapter 2. The iDecell + Comp C group showed robust nerve regeneration comparable to that of an unprocessed nerve graft as shown in Figure 4.12. This result is very encouraging as the decellularized nerve grafts supplemented with Comp C have comparable amount of regeneration to the clinical "gold standard". The data obtained from iDecell + Comp C group is promising and expands the opportunity to try other compounds to improve long gap regeneration using iDecell grafts.

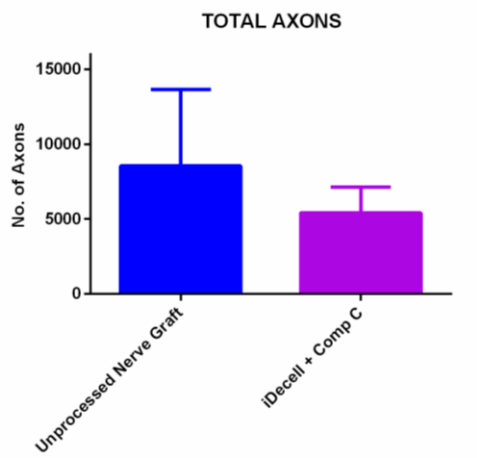

Figure 4.12 Comparison of axon count between Unprocessed nerve graft and iDecell + Comp C group

4.4 Summary

In summary, the detergent-free decellularized nerve graft presented in this work proved to be superior to the current state of art (detergent-processed nerve grafts), but still inferior to the gold standard (unprocessed nerve grafts). We have developed an optimized detergent-free decellularization method to obtain nerve grafts with structural and biological properties necessary for nerve regeneration. We demonstrated that the decellularized nerve grafts successfully promoted functional nerve regeneration across a 35 mm long gap defect. We also showed that drug-supplemented decellularized nerve grafts (iDecell + Comp C) regenerated more than twice the number of axons compared to the unsupplemented grafts (iDecell), and had statistically equivalent results to unprocessed nerve graft "gold standard". Overall, our work demonstrates that optimization of decellularization protocols combined with rational selection of drug supplements can elicit functional nerve regeneration, comparable to that of an unprocessed nerve graft.

CHAPTER 5

CONCLUSION AND FUTURE OUTLOOK

5.1 Summary

The goal of this research project was to develop detergent-free decellularized nerve grafts for reconstruction of long gap nerve defects. We developed a detergent-free decellularization technique based on *in vitro* Wallerian degeneration and obtained functional regeneration across a 35 mm long gap injury. Despite having regeneration across a previously untested injury using decellularized nerve grafts, limited axonal growth required further exploration to improve nerve regeneration. We developed a growth vs. no-growth nerve injury model that allowed us to study the difference in molecular signature between a regenerative and a non-regenerative injury, which was used to rationally select compounds that would aid nerve regeneration. Using the newly described molecular profile, we selected three such compounds that enhanced axonal growth in regenerative settings and promoted nerve regeneration across a critical nerve injury. To improve regeneration in detergent-free decellularized nerve grafts, we optimized the processing technique and examined nerve regeneration with or without supplementing compounds that enhanced nerve regeneration. We successfully demonstrated that one of the three compounds, when delivered along with the improved detergent-free decellularized nerve grafts, promoted regeneration comparable to the clinical gold standard. The work presented here has numerous advantages over existing detergent processed grafts and has high potential for clinical use.

5.2 Limitations and Future Work

The research presented here has potential for use in clinical settings, but there is still room for improvement before implementation in real case scenarios. We have planned longer time point studies for definitively comparing functional recovery in all the implanted groups. To

evaluate the immunogenic properties, xenograft models have to be tested. To date, a sustained delivery mechanism to deliver selected compounds has not been tested, and future studies will be performed by using multiple drug delivery systems for sustained drug delivery. Finally, confirmation of the results in a large animal model is necessary prior to introduction to the clinic.

REFERENCES

Abercrombie M, Johnson ML (1946) Quantitative histology of Wallerian degeneration: I. Nuclear population in rabbit sciatic nerve. J Anat 80:37–50.

Battiston B, Geuna S, Ferrero M, Tos P (2005) Nerve repair by means of tubulization: literature review and personal clinical experience comparing biological and synthetic conduits for sensory nerve repair. Microsurgery 25:258–267.

Belkas JS, Shoichet MS, Midha R (2004) Peripheral nerve regeneration through guidance tubes. Neurol Res 26:151–160.

Bellamkonda R V (2006) Peripheral nerve regeneration: an opinion on channels, scaffolds and anisotropy. Biomaterials 27:3515–3518.

Berrocal Y a, Almeida VW, Levi AD (2013) Limitations of nerve repair of segmental defects using acellular conduits. J Neurosurg 119:733–738.

Blondet B, Carpentier G, Lafdil F, Courty J (2005) Pleiotrophin cellular localization in nerve regeneration after peripheral nerve injury. J Histochem Cytochem 53:971–977.

Boyd KU, Nimigan AS, Mackinnon SE (2011) Nerve reconstruction in the hand and upper extremity. Clin Plast Surg 38:643–660.

Brück W (1997) The role of macrophages in Wallerian degeneration. Brain Pathol 7:741–752.

Burnett MG, Zager EL (2004) Pathophysiology of peripheral nerve injury: a brief review. Neurosurg Focus 16:E1.

Buttermore ED, Thaxton CL, Bhat M a (2013) Organization and maintenance of molecular domains in myelinated axons. J Neurosci Res 91:603–622.

Campbell WW (2008) Evaluation and management of peripheral nerve injury. Clin Neurophysiol 119:1951–1965.

Cho MS, Rinker BD, Weber R V, Chao JD, Ingari J V, Brooks D, Buncke GM (2012) Functional outcome following nerve repair in the upper extremity using processed nerve allograft. J Hand Surg Am 37:2340–2349.

Coleman MP, Freeman MR (2010) Wallerian degeneration, wld(s), and nmnat. Annu Rev Neurosci 33:245–267.

Crapo PM, Gilbert TW, Badylak SF (2011) An overview of tissue and whole organ decellularization processes. Biomaterials 32:3233–3243.

Damsky CH, Werb Z (1992) Signal transduction by integrin receptors for extracellular matrix: cooperative processing of extracellular information. Curr Opin Cell Biol 4:772–781.

Dowsing BJ, Morrison W a, Nicola N a, Starkey GP, Bucci T, Kilpatrick TJ (1999) Leukemia inhibitory factor is an autocrine survival factor for Schwann cells. J Neurochem 73:96–104.

Drapeau J, El-Helou V, Clement R, Bel-Hadj S, Gosselin H, Trudeau L-E, Villeneuve L, Calderone A (2005) Nestin-expressing neural stem cells identified in the scar following myocardial infarction. J Cell Physiol 204:51–62.

Ehretsman RL, Novak CB, Mackinnon SE (1999) Subjective recovery of nerve graft donor site. Ann Plast Surg 43:606–612.

Evans GR (2001) Peripheral nerve injury: a review and approach to tissue engineered constructs. Anat Rec 263:396–404.

Evans P, Mackinnon S, Levi A (1998) Cold preserved nerve allografts: changes in basement membrane, viability, immunogenicity, and regeneration. … nerve:1507–1522.

Fernandes KJL, McKenzie I a, Mill P, Smith KM, Akhavan M, Barnabé-Heider F, Biernaskie J, Junek A, Kobayashi NR, Toma JG, Kaplan DR, Labosky P a, Rafuse V, Hui C-C, Miller FD (2004) A dermal niche for multipotent adult skin-derived precursor cells. Nat Cell Biol 6:1082–1093.

Fine EG, Decosterd I, Papalozos M, Zurn AD, Aebischer P (2002) GDNF and NGF released by synthetic guidance channels support sciatic nerve regeneration across a long gap. Eur J Neurosci 15:589–601.

Frostick SP, Yin Q, Kemp GJ (1998) Schwann cells, neurotrophic factors, and peripheral nerve regeneration. Microsurgery 18:397–405.

Garde K, Keefer E, Botterman B, Galvan P, Romero MI (2009) Early interfaced neural activity from chronic amputated nerves. Front Neuroeng 2:5.

Gaudet AD, Popovich PG, Ramer MS (2011) Wallerian degeneration: gaining perspective on inflammatory events after peripheral nerve injury. J Neuroinflammation 8:110.

Gijtenbeek JM, van den Bent MJ, Vecht CJ (1999) Cyclosporine neurotoxicity: a review. J Neurol 246:339–346.

Griffin JW, George R, Lobato C, Tyor WR, Yan LC, Glass JD (1992) Macrophage responses and myelin clearance during Wallerian degeneration: relevance to immune-mediated demyelination. J Neuroimmunol 40:153–165.

Guo Y, Chen G, Tian G, Tapia C (2013) Sensory recovery following decellularized nerve allograft transplantation for digital nerve repair. J Plast Surg Hand Surg:1–3.

Haase SC, Rovak JM, Dennis RG, Kuzon WM, Cederna PS (2003) Recovery of muscle contractile function following nerve gap repair with chemically acellularized peripheral nerve grafts. J Reconstr Microsurg 19:241–248.

Henderson C, Phillips H, Pollock R, Davies A, Lemeulle C, Armanini M, Simmons L, Moffet B, Vandlen R, Simpson LC [corrected to Simmons L, Et A (1994) GDNF: a potent survival factor for motoneurons present in peripheral nerve and muscle. Science (80-) 266:1062–1064.

Hirata K, Mitoma H, Ueno N, He JW, Kawabuchi M (1999) Differential response of macrophage subpopulations to myelin degradation in the injured rat sciatic nerve. J Neurocytol 28:685–695.

HOBSON MI, GREEN CJ, TERENGHI G (2000) VEGF enhances intraneural angiogenesis and improves nerve regeneration after axotomy. J Anat 197:591–605.

Hontanilla B, Aubá C, Arcocha J, Gorría O (2006) Nerve regeneration through nerve autografts and cold preserved allografts using tacrolimus (FK506) in a facial paralysis model: a topographical and neurophysiological study in monkeys. Neurosurgery 58:768–79; discussion 768–79.

Hudson TW, Liu SY, Schmidt CE (2004) Engineering an improved acellular nerve graft via optimized chemical processing. Tissue Eng 10:1346–1358.

Hunter D a, Moradzadeh A, Whitlock EL, Brenner MJ, Myckatyn TM, Wei CH, Tung THH, Mackinnon SE (2007) Binary imaging analysis for comprehensive quantitative histomorphometry of peripheral nerve. J Neurosci Methods 166:116–124.

Ide C, Tohyama K, Yokota R, Nitatori T, Onodera S (1983) Schwann cell basal lamina and nerve regeneration. Brain Res 288:61–75.

Joseph NM, Mukouyama Y-S, Mosher JT, Jaegle M, Crone SA, Dormand E-L, Lee K-F, Meijer D, Anderson DJ, Morrison SJ (2004) Neural crest stem cells undergo multilineage differentiation in developing peripheral nerves to generate endoneurial fibroblasts in addition to Schwann cells. Development 131:5599–5612.

Kale SS, Glaus SW, Yee A, Nicoson MC, Hunter D a, Mackinnon SE, Johnson PJ (2011) Reverse end-to-side nerve transfer: from animal model to clinical use. J Hand Surg Am 36:1631–1639.e2.

Karabekmez FE, Duymaz A, Moran SL (2009) Early clinical outcomes with the use of decellularized nerve allograft for repair of sensory defects within the hand. Hand (N Y) 4:245–249.

Katayama Y, Montenegro R, Freier T, Midha R, Belkas JS, Shoichet MS (2006) Coil-reinforced hydrogel tubes promote nerve regeneration equivalent to that of nerve autografts. Biomaterials 27:505–518.

Kawamura DH, Johnson PJ, Moore AM, Magill CK, Hunter D a, Ray WZ, Tung THH, Mackinnon SE (2010) Matching of motor-sensory modality in the rodent femoral nerve model shows no enhanced effect on peripheral nerve regeneration. Exp Neurol 223:496–504.

King R (2013) Microscopic anatomy: normal structure. Handb Clin Neurol 115:7–27.

Komiyama T, Nakao Y, Toyama Y, Asou H, Vacanti C a, Vacanti MP (2003) A novel technique to isolate adult Schwann cells for an artificial nerve conduit. J Neurosci Methods 122:195–200.

Lu X, Tao Y, Li L (2012) Prospective use of skin-derived precursors in neural regeneration. Chin Med J (Engl) 125:4488–4496.

Lundborg G, Dahlin LB, Danielsen N, Gelberman RH, Longo FM, Powell HC, Varon S (1982a) Nerve regeneration in silicone chambers: influence of gap length and of distal stump components. Exp Neurol 76:361–375.

Lundborg G, Longo FM, Varon S (1982b) Nerve regeneration model and trophic factors in vivo. Brain Res 232:157–161.

Lutz BS, Chuang DC, Chuang SS, Hsu JC, Ma SF, Wei FC (2000) Nerve transfer to the median nerve using parts of the ulnar and radial nerves in the rabbit--effects on motor recovery of the median nerve and donor nerve morbidity. J Hand Surg Br 25:329–335.

Mackinnon S, Hudson A, Falk R, Bilbao J (1982) Nerve allograft response: a quantitative immunological study. Neurosurgery.

Mackinnon SE, Hudson AR, Bain JR, Falk RE, Hunter DA (1987) The peripheral nerve allograft: an assessment of regeneration in the immunosuppressed host. Plast Reconstr Surg 79:436–446.

Madison RD, Da Silva CF, Dikkes P (1988) Entubulation repair with protein additives increases the maximum nerve gap distance successfully bridged with tubular prostheses. Brain Res 447:325–334.

Magill CK, Tong A, Kawamura D, Hayashi A, Hunter D a, Parsadanian A, Mackinnon SE, Myckatyn TM (2007) Reinnervation of the tibialis anterior following sciatic nerve crush injury: a confocal microscopic study in transgenic mice. Exp Neurol 207:64–74.

Mi R, Chen W, Höke A (2007) Pleiotrophin is a neurotrophic factor for spinal motor neurons. Proc Natl Acad Sci U S A 104:4664–4669.

Midha R, Mackinnon SE, Evans PJ, Best TJ, Hare GM, Hunter DA, Falk-Wade JA (1993) Comparison of regeneration across nerve allografts with temporary or continuous cyclosporin A immunosuppression. J Neurosurg 78:90–100.

Mokarram N, Merchant A, Mukhatyar V, Patel G, Bellamkonda R V (2012) Effect of modulating macrophage phenotype on peripheral nerve repair. Biomaterials 33:8793–8801.

Moore AM, Kasukurthi R, Magill CK, Farhadi HF, Borschel GH, Mackinnon SE (2009) Limitations of conduits in peripheral nerve repairs. Hand (N Y) 4:180–186.

Nagao RJ, Lundy S, Khaing ZZ, Schmidt CE (2011) Functional characterization of optimized acellular peripheral nerve graft in a rat sciatic nerve injury model. Neurol Res 33:600–608.

Navarro X, Vivó M, Valero-Cabré A (2007) Neural plasticity after peripheral nerve injury and regeneration. Prog Neurobiol 82:163–201.

Neubauer D, Graham JBJ, Muir D (2007) Chondroitinase treatment increases the effective length of acellular nerve grafts. Exp Neurol 207:163–170.

Noble J, Munro CA, Prasad VS, Midha R (1998) Analysis of upper and lower extremity peripheral nerve injuries in a population of patients with multiple injuries. J Trauma 45:116–122.

Olsson T, Kristensson K, Ljungdahl A, Maehlen J, Holmdahl R, Klareskog L (1989) Gamma-interferon-like immunoreactivity in axotomized rat motor neurons. J Neurosci 9:3870–3875.

Pfister BJ, Gordon T, Loverde JR, Kochar AS, Mackinnon SE, Cullen DK (2011) Biomedical engineering strategies for peripheral nerve repair: surgical applications, state of the art, and future challenges. Crit Rev Biomed Eng 39:81–124.

Porayko MK, Textor SC, Krom RA, Hay JE, Gores GJ, Richards TM, Crotty PH, Beaver SJ, Steers JL, Wiesner RH (1994) Nephrotoxic effects of primary immunosuppression with FK-506 and cyclosporine regimens after liver transplantation. Mayo Clin Proc 69:105–111.

Reichert F, Saada a, Rotshenker S (1994) Peripheral nerve injury induces Schwann cells to express two macrophage phenotypes: phagocytosis and the galactose-specific lectin MAC-2. J Neurosci 14:3231–3245.

Reyes O, Sosa I, Kuffler DPD (2005) Promoting neurological recovery following a traumatic peripheral nerve injury. P R Health Sci J 24:215–223.

Reynolds ML, Fitzgerald M, Benowitz LI (1991) GAP-43 expression in developing cutaneous and muscle nerves in the rat hindlimb. Neuroscience 41:201–211.

Rivlin M, Sheikh E, Isaac R, Beredjiklian PK (2010) The role of nerve allografts and conduits for nerve injuries. Hand Clin 26:435–46, viii.

Santosa KB, Jesuraj NJ, Viader A, Macewan M, Newton P, Hunter D a, Mackinnon SE, Johnson PJ (2013) Nerve allografts supplemented with schwann cells overexpressing glial-cell-line-derived neurotrophic factor. Muscle Nerve 47:213–223.

Seddon HJ (1943) Three types of brain injury. Brain 66:237–288.

Shen ZL, Berger a, Hierner R, Allmeling C, Ungewickell E, Walter GF (2001) A Schwann cell-seeded intrinsic framework and its satisfactory biocompatibility for a bioartificial nerve graft. Microsurgery 21:6–11.

Siemionow M, Bozkurt M, Zor F (2010) Regeneration and repair of peripheral nerves with different biomaterials: review. Microsurgery 30:574–588.

Skene J, Jacobson R, Snipes G, McGuire C, Norden J, Freeman J (1986) A protein induced during nerve growth (GAP-43) is a major component of growth-cone membranes. Science (80-) 233:783–786.

Sondell M, Lundborg G, Kanje M (1999) Vascular endothelial growth factor has neurotrophic activity and stimulates axonal outgrowth, enhancing cell survival and Schwann cell proliferation in the peripheral nervous system. J Neurosci 19:5731–5740.

Spreca a., Rambotti MG, Rende M, Saccardi C, Aisa MC, Giambanco I, Donato R (1989) Immunocytochemical localization of S-100b protein in degenerating and regenerating rat sciatic nerves. J Histochem Cytochem 37:441–446.

Spreyer P, Schaal H, Kuhn G, Rothe T, Unterbeck a, Olek K, Müller HW (1990) Regeneration-associated high level expression of apolipoprotein D mRNA in endoneurial fibroblasts of peripheral nerve. EMBO J 9:2479–2484.

Stoll G, Griffin JW, Li CY, Trapp BD (1989) Wallerian degeneration in the peripheral nervous system: participation of both Schwann cells and macrophages in myelin degradation. J Neurocytol 18:671–683.

Stoll G, Jander S, Myers RR (2002) Degeneration and regeneration of the peripheral nervous system: From Augustus Waller's observations to neuroinflammation. J Peripher Nerv Syst 7:13–27.

Stoll G, Müller HW (1999) Nerve injury, axonal degeneration and neural regeneration: basic insights. Brain Pathol 9:313–325.

Strauch B, Rodriguez DM, Diaz J, Yu HL, Kaplan G, Weinstein DE (2001) Autologous Schwann cells drive regeneration through a 6-cm autogenous venous nerve conduit. J Reconstr Microsurg 17:589–95; discussion 596–7.

Sunderland IRP, Brenner MJ, Singham J, Rickman SR, Hunter D a., Mackinnon SE (2004) Effect of Tension on Nerve Regeneration in Rat Sciatic Nerve Transection Model. Ann Plast Surg 53:382–387.

Sunderland S (1951) A classification of peripheral nerve injuries producing loss of function. Brain 74:491–516.

Sunderland S (1990) The anatomy and physiology of nerve injury. Muscle Nerve 13:771–784.

Szynkaruk M, Kemp SWP, Wood MD, Gordon T, Borschel GH (2013) Experimental and clinical evidence for use of decellularized nerve allografts in peripheral nerve gap reconstruction. Tissue Eng Part B Rev 19:83–96.

Taskinen HS, Olsson T, Bucht a, Khademi M, Svelander L, Röyttä M (2000) Peripheral nerve injury induces endoneurial expression of IFN-gamma, IL-10 and TNF-alpha mRNA. J Neuroimmunol 102:17–25.

Terenghi G (1999) Peripheral nerve regeneration and neurotrophic factors. J Anat 194:1–14.

Thomas PK (1963) The connective tissue of peripheral nerve: an electron microscope study. J Anat 97:35–44.

Tofaris GK, Patterson PH, Jessen KR, Mirsky R (2002) Denervated Schwann cells attract macrophages by secretion of leukemia inhibitory factor (LIF) and monocyte chemoattractant protein-1 in a process regulated by interleukin-6 and LIF. J Neurosci 22:6696–6703.

Toma JG, Akhavan M, Fernandes KJ, Barnabé-Heider F, Sadikot A, Kaplan DR, Miller FD (2001) Isolation of multipotent adult stem cells from the dermis of mammalian skin. Nat Cell Biol 3:778–784.

Tong XJ, Hirai K, Shimada H, Mizutani Y, Izumi T, Toda N, Yu P (1994) Sciatic nerve regeneration navigated by laminin-fibronectin double coated biodegradable collagen grafts in rats. Brain Res 663:155–162.

Tötösy de Zepetnek JE, Zung H V, Erdebil S, Gordon T (1992) Innervation ratio is an important determinant of force in normal and reinnervated rat tibialis anterior muscles. J Neurophysiol 67:1385–1403.

Vasudevan S, Yan J-G, Zhang L-L, Matloub HS, Cheng JJ (2013) A rat model for long-gap peripheral nerve reconstruction. Plast Reconstr Surg 132:871–876.

Wang G-Y, Hirai K-I, Shimada H, Taji S, Zhong S-Z (1992) Behavior of axons, Schwann cells and perineurial cells in nerve regeneration within transplanted nerve grafts: effects of anti-laminin and anti-fibronectin antisera. Brain Res 583:216–226.

Whitlock EL, Tuffaha SH, Luciano JP, Yan Y, Hunter D a, Magill CK, Moore AM, Tong AY, Mackinnon SE, Borschel GH (2009) Processed allografts and type I collagen conduits for repair of peripheral nerve gaps. Muscle Nerve 39:787–799.

Wilhelm JC, Xu M, Cucoranu D, Chmielewski S, Holmes T, Lau KS, Bassell GJ, English AW (2012) Cooperative roles of BDNF expression in neurons and Schwann cells are modulated by exercise to facilitate nerve regeneration. J Neurosci 32:5002–5009.

Williams LR, Longo FM, Powell HC, Lundborg G, Varon S (1983) Spatial-temporal progress of peripheral nerve regeneration within a silicone chamber: parameters for a bioassay. J Comp Neurol 218:460–470.

Witoonchart K, Leechavengvongs S, Uerpairojkit C, Thuvasethakul P, Wongnopsuwan V (2003) Nerve transfer to deltoid muscle using the nerve to the long head of the triceps, part I: an anatomic feasibility study. J Hand Surg Am 28:628–632.

Yannas I V, Zhang MEI, Spilker MH (2007) Standardized criterion to analyze and directly compare various materials and models for peripheral nerve. 18:943–966.

Ydens E, Cauwels A, Asselbergh B, Goethals S, Peeraer L, Lornet G, Almeida-Souza L, Van Ginderachter J a, Timmerman V, Janssens S (2012) Acute injury in the peripheral nervous system triggers an alternative macrophage response. J Neuroinflammation 9:176.

Zhang J-Y, Luo X-G, Xian CJ, Liu Z-H, Zhou X-F (2000) Endogenous BDNF is required for myelination and regeneration of injured sciatic nerve in rodents. Eur J Neurosci 12:4171–4180.

BIOGRAPHICAL INFORMATION

Srikanth Vasudevan grew up in New Delhi, India. After completing high school, he obtained a bachelor's degree in Biomedical Instrumentation from Dr. M.G.R. Educational and Research Institute, Chennai, India. During the course of his undergraduate education, he completed internship with Carl Zeiss India Ltd. He worked in Indus Medical Instruments Pvt. Ltd after completing his Bachelor's degree, where he developed immense interest in Biomedical research. To further explore research opportunities, he joined Master of Science in Biomedical Engineering at the University of Texas at Arlington and worked on various *in vitro* assays for neuroscience and oncology research. His interest in neuroscience research allowed him to continue his education and pursue Doctor of Philosophy in Biomedical Engineering, during which he completed an internship at Plexon Inc., Dallas. He joined Dr. Jonathan Cheng's lab at the University of Texas Southwestern Medical Center in 2011, where he obtained insight on clinically relevant peripheral nerve research. He was also mentored by Dr. Edward Keefer, who played an integral part in shaping his research skills. It is his ultimate aim to continue clinically relevant research for improving quality of patient life.